

General Disclaimer

One or more of the Following Statements may affect this Document

- This document has been reproduced from the best copy furnished by the organizational source. It is being released in the interest of making available as much information as possible.
- This document may contain data, which exceeds the sheet parameters. It was furnished in this condition by the organizational source and is the best copy available.
- This document may contain tone-on-tone or color graphs, charts and/or pictures, which have been reproduced in black and white.
- This document is paginated as submitted by the original source.
- Portions of this document are not fully legible due to the historical nature of some of the material. However, it is the best reproduction available from the original submission.

PREDICTING THE DYE LAYER DENSITIES OF COLOR INFRARED
TRANSPARENCIES

With an Addendum

COLOR INFRARED PHOTOGRAPHY THROUGH SPACECRAFT WINDOWS

By

Robert W. Pease

University of California, Riverside

Submitted to the
Manned Spacecraft Center
at the request of

Arch C. Gerlach
United States Geological Survey

FACILITY FORM 602

N69-35733 (ACCESSION NUMBER)	_____ (THRU)
31 (PAGES)	1 (CODE)
NASA-CR-104208 (NASA CR OR TMX OR AD NUMBER)	14 (CATEGORY)

06-00148

PREDICTING THE RELATIVE DYE LAYER DENSITIES OF COLOR INFRARED
TRANSPARENCIES

Occasions arise when it is desirable to predict in advance the probable success of color infrared film to yield a meaningful red record. Whether or not to use the film or the intelligent choice of appropriate minus-visual auxiliary filters to combat the effects of altitude (Pease and Bowden, 1968) will save time and funds when planning a CIR photo mission.

The need for prediction arises from the fact that the infrared recording or cyan-forming layer in the film has been designed with something less than half the sensitivity of either of the other two layers. Thus exposure spectrally available to this layer must be significantly greater than that to either of the other layers in order that cyan density in the finished transparency be the lowest of the three, a condition necessary for a red balance. This need is in contradiction to sunlight as an illuminant for the major sensitivity of the cyan-forming layer is to the weakest part of the sunlight energy distribution in the CIR waveband, 500-900 nanometers.

In making an assessment of relative dye layer densities, it is necessary to know the spectral distribution of energy reaching the film. By a method later described, this can be plotted on a conventional D Log E diagram for the film (Kodak Ektrachrome Infrared Aero, Type 8443) to determine densities. Energy reaching the film will be the energy reaching the camera, attenuated by the combined transmittances of all filters used with the CIR system. When photos are to be taken through spacecraft windows, the transmittance characteristics of the window and its coatings must be considered as another attenuating filter.

The energy reaching a high altitude photo platform will have a spectral distribution that will consist of the reflection from the ground target, attenuated somewhat in the near infrared by water vapor in the light path, to which has been added the energy of air luminance from the atmospheric upscatter of sunlight. The reflection or energy leaving the target will have a spectral distribution that is the sunlight illumination molded by the reflectance of the target materials. Reflectance is a property of the target that is independent of the nature of the illumination (Fig. 1).

THE METHOD

A graphical method has been used in making density determinations. This involves (1) plotting the spectral curve of energy reaching the film, (2) weighting the energy available in discrete wave zones with an effectiveness factor for the sensitivity in the zone of each dye layer, and (3) plotting the summations of exposure of each dye layer on a conventional $D \log E$ sensitometric diagram for Type 8443 film.

Basic details of the procedure are illustrated with the aid of the following graphical representations. With one exception, reflection curves were actually measured in nature at Southern California sites with the aid of an ISCO Model SR spectroradiometer.

Some Sensitometric Considerations

To facilitate the calculation of exposure, the CIR spectrum (500-900 nm.) was divided into eight 50 nm. wave zones. Each film layer responds to a greater or lesser extent to several of these zones. For the cyan-forming layer, there is some exposure in all eight, although the preponderance occurs between 700 and 900 nm.

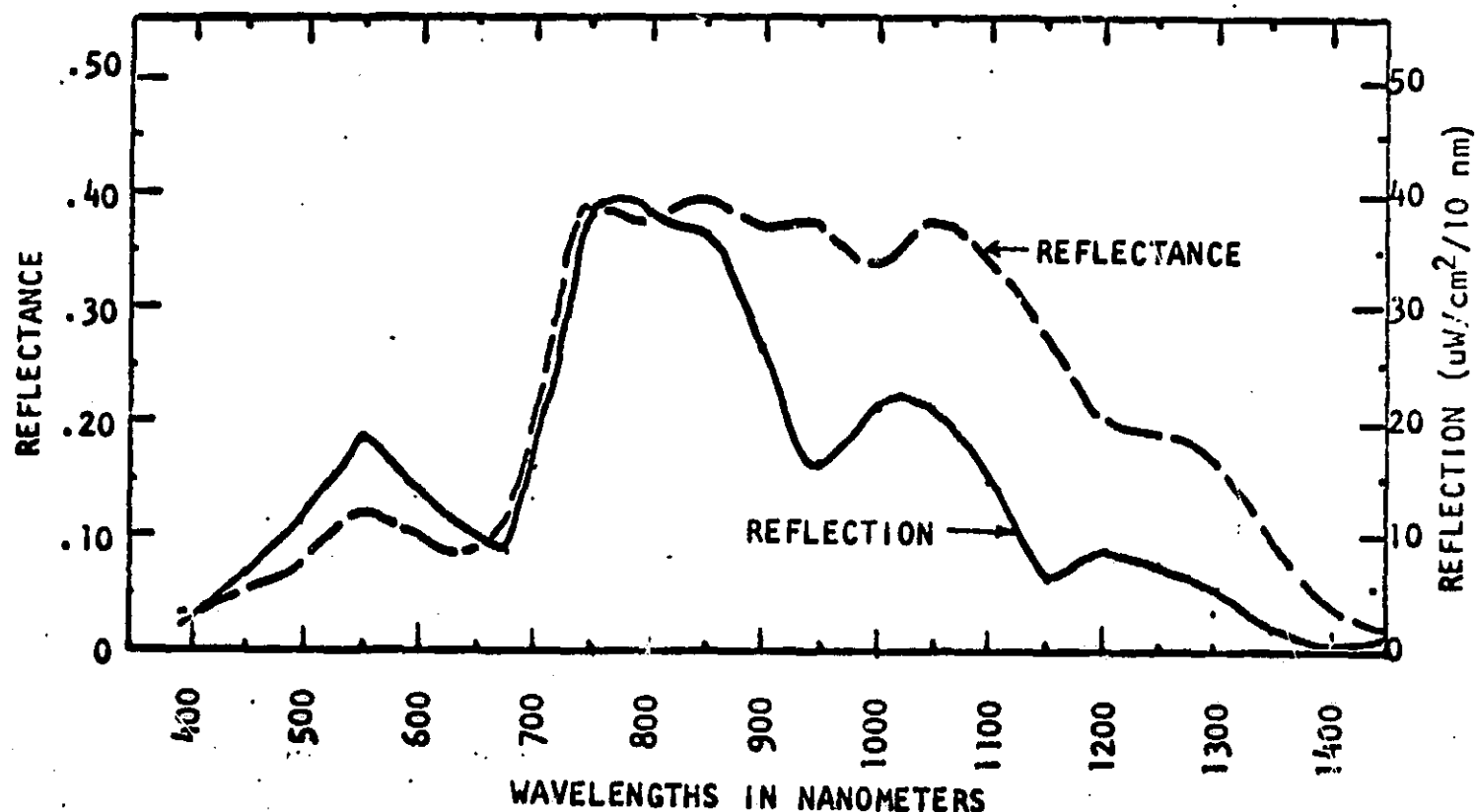


Fig. 1. Reflection vs. reflectance. Reflectance is a property of a target that is independent of the spectral distribution of illumination. For any wavelength, it is the fraction of the incident energy that will be reflected. In this manner, reflectance molds the spectral curve of illumination into the curve of reflection or energy that leaves the target.

This figure shows curves of reflectance and reflection superimposed in such a way that values coincide at 750 nm. It is to be noted that the sunlight peak near 550 nm. causes reflection to be higher in the visual, but to drop off or be lower in the near infrared.

For a specific target, the curve of energy reflected will vary with the nature of the illumination according to atmospheric conditions and the altitude of the sun. A typical solar curve, measured in Riverside, California, is used for the following illustrative graphs (Fig. 5).

To create the weighting factors of energy effectiveness for each layer in each zone, a linear plot was made of the spectral distribution of film layer sensitivities (Fig. 2) based upon curves presented by Tarkington and Sorem (1963) and Fritz (1967). Since the curves are essentially the transparencies of each layer for a given exposure, areas within the curves will be proportional to sensitivity. The weighting factor is the fraction of the total area of a curve that occurs in a 50 nm. zone. This corresponds to the fraction of the total exposure that occurs in the zone when exposure is from a neutral light source.

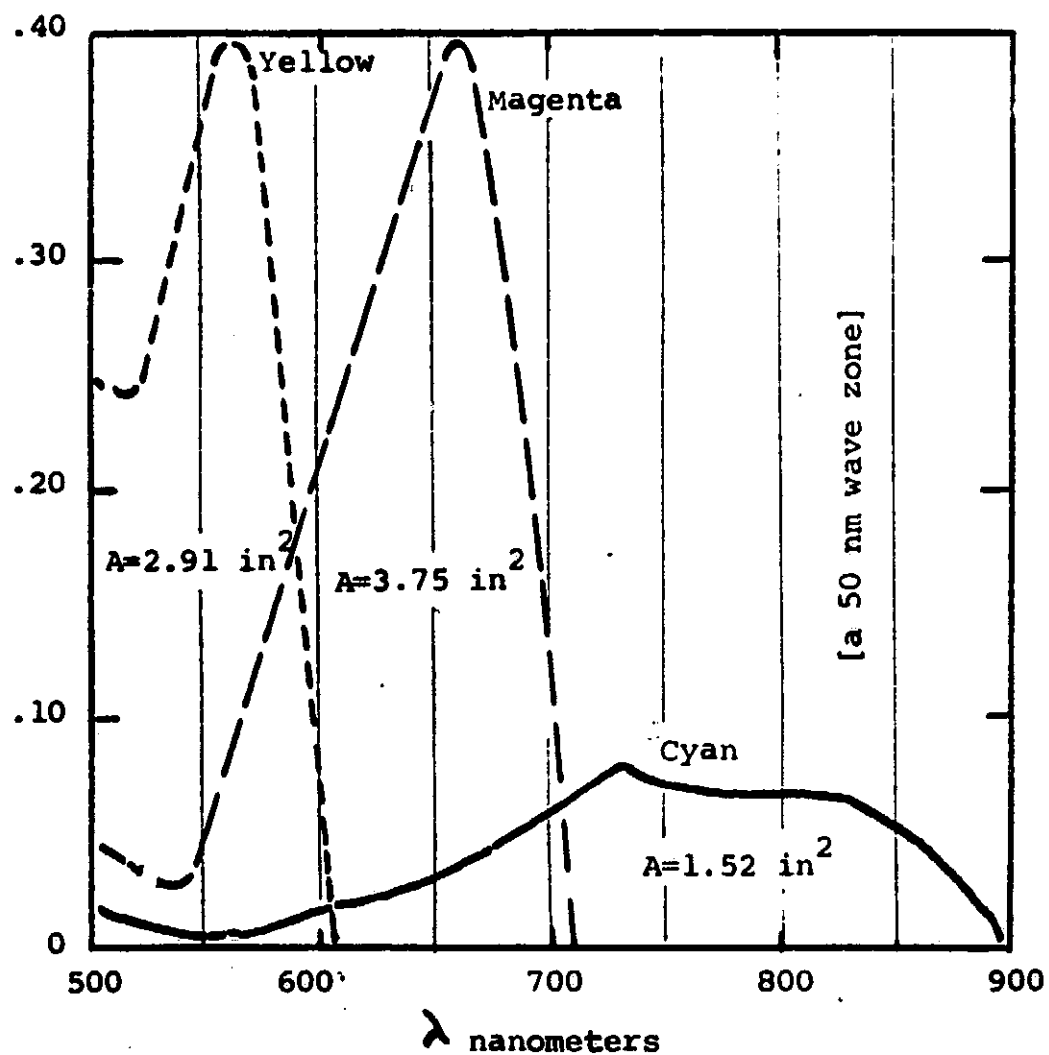
When the areas of the spectral sensitivity curves were related to each other, it was found they did not agree with the $D \log E$ curves presented by Fritz (1967) but were in agreement with those of Tarkington and Sorem (1963). It was presumed that a drafting error had occurred in the preparation of Fritz's curves, and so those of Tarkington and Sorem were used. These are the sensitometric curves published at the time Type 8443 film was introduced.

Although exposure is expressed as a logarithmic value, a linear scale is included for exposure on the following graphs. Logs of the exposures can be plotted on a linear scale with perhaps greater accuracy than when placing exposure directly onto a logarithmic grid.

Figure 3 plots densities for pine needles as a close-range plant target. Figure 4 shows the worksheet that is used to weigh exposure effectiveness in each of the 50 nm. zones. These two figures illustrate the method employed.

Figure 2.

LINEAR PLOTS OF FILM LAYER SENSITIVITIES OF TYPE 8443 CIR FILM



$$\frac{Y}{C} = 1.91$$

$$\frac{M}{C} = 2.46$$

$$\frac{C}{Y} = .52$$

$$\frac{C}{M} = .405$$

EXPOSURE EFFECTIVENESS OF FILM LAYERS FOR 50 NANOMETER BANDS

Expressed as a fraction of the total sensitivity of the film layer

<u>nm</u>	<u>Yellow</u>	<u>Magenta</u>	<u>Cyan</u>
500-550	.47	.04	.03
550-600	.50	.17	.03
600-650	.03	.38	.07
650-700	--	.40	.14
700-750	--	.01	.24
750-800	--	--	.21
800-850	--	--	.20
850-900	--	--	.08

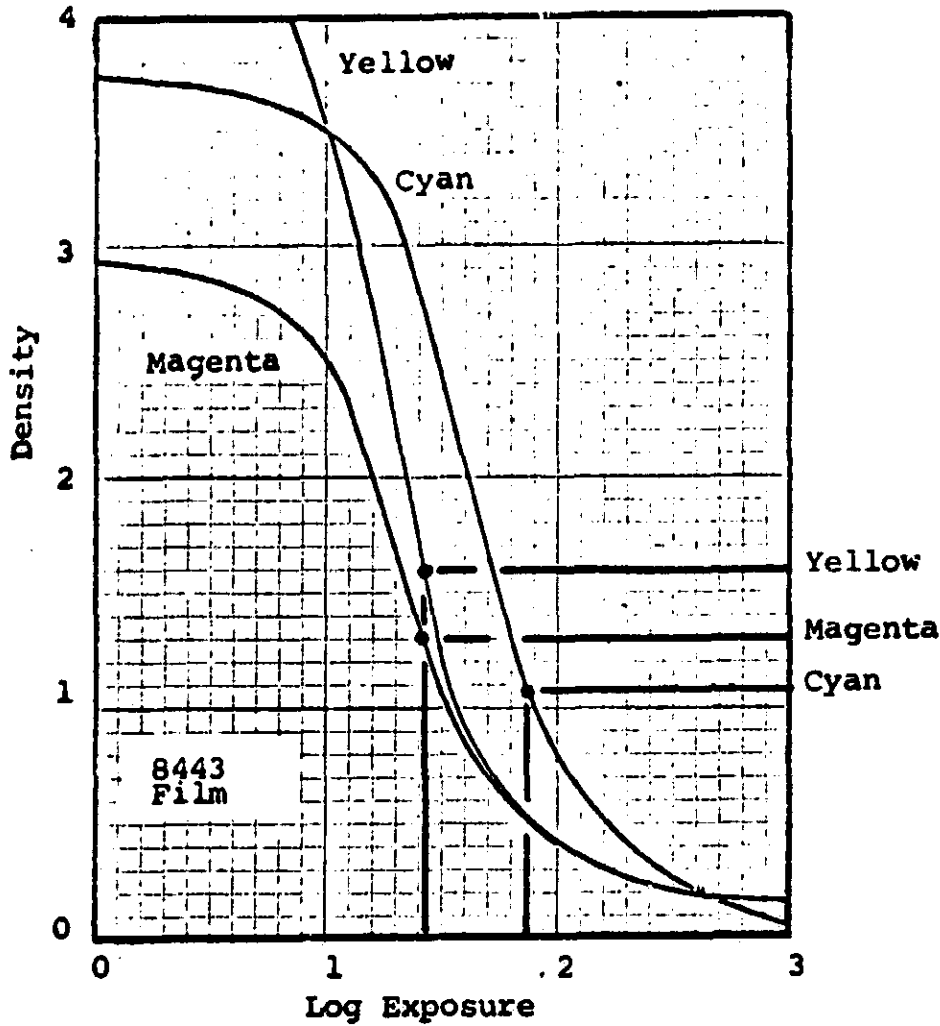
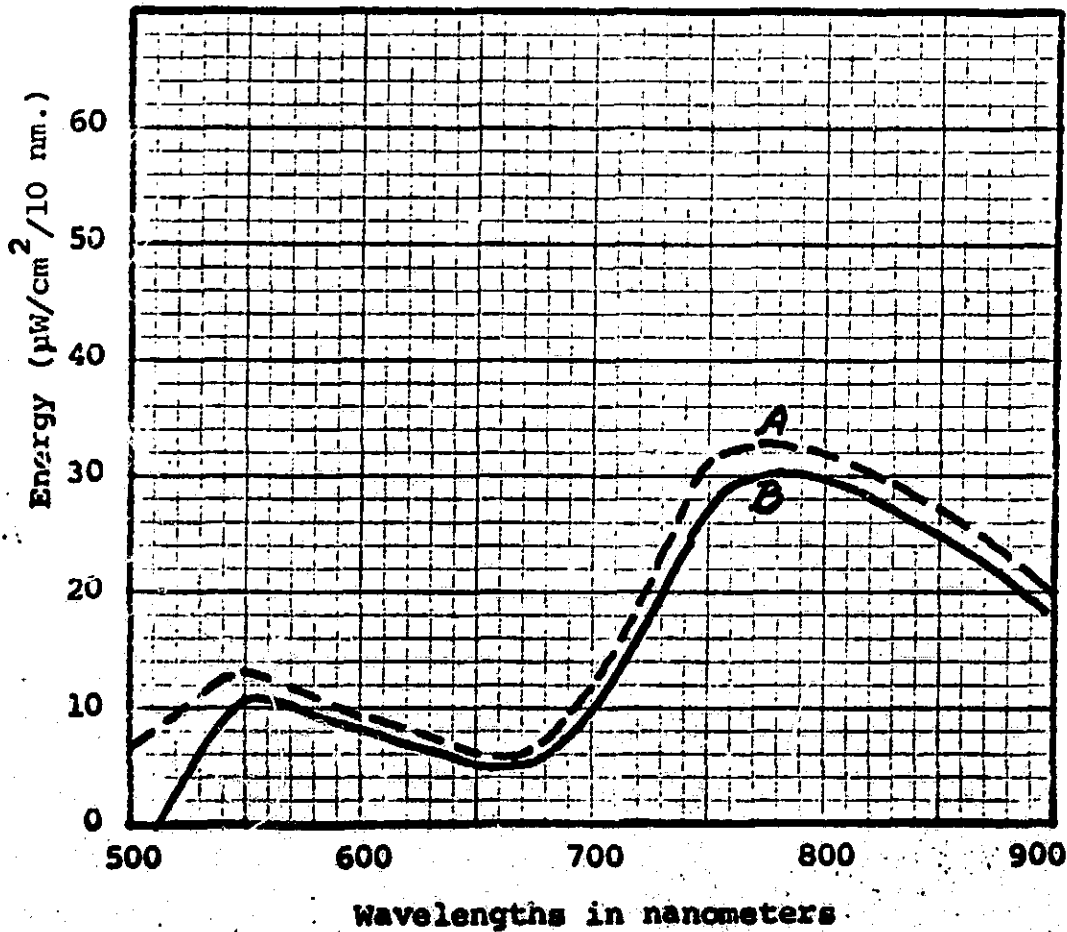


Figure 3. Pine needle reflection at close range, attenuated at camera only by the minus-blue (15) filter of the CIR system.

A= 10.6 24.0 16.0 15.0 45.0 73.6 68.0 53.0



A=Pine needle reflection under typical sunlight.
 B=Energy reaching film -- A attenuated by 15 filter.

A SAMPLE PLOTTING

Curve A in the lower graph of Figure 3 is the reflection from pine needles measured directly in energy terms with an ISCO spectroradiometer. A similar curve could have been constructed by integrating the reflectance curve for the pine needles with an appropriate sunlight illumination curve. Curve A is the energy reaching the camera. Curve B plots the energy after it has been attenuated by a Wratten 15 filter, the basic minus-blue filter for the CIR system. This is the energy actually reaching the film.

The area within Curve B in each of the 50 nm wave zones is then measured. The number at the top of the column is the number of $.01 \text{ in}^2$ squares within the curve in the 50 nm. zone. These areas are proportional to the energy available to the film in each zone. A 50 nm. zone appears to be a good compromise that permits speed in computation and a desirable order of accuracy.

The waveband areas are entered on a worksheet (Fig. 4) where they are used as functions with the exposure effectiveness weighting factors, the sheet provides, to calculate the effective exposure of each film layer in each zone. The summations of the effective exposure for each layer is then multiplied by a factor (X) that will cause the D log E plottings to fall on the straight-line portions of the curves. In general, a factor that places the cyan exposure between 60 and 80 will give a good result. Of course, the same factor must be applied to summations for each of the layers. Logarithms of the exposures are ascertained and density points are plotted on the D log E diagram.

In the pine needle example, the cyan layer density is only moderately lower than those of the other layers. This is compatible with experience

with CIR photos of this target using only minus-blue filtration. Only a slight lowering of the IR/Visual reflectance ratio of a coniferous target causes cyan to predominate and the red record to be lost. This has made the CIR system useful in studying vigor and disease in coniferous forests. For a target with a higher IR/Visual reflectance ratio, such as broadleaf forest in new foliage or grass, the cyan density would be markedly lower.

HIGH ALTITUDE USE

Although the pine needle target will yield a red record at close range it will not do so with the conventional CIR system at high altitudes. Deterioration of the red results from (1) a moderate amount of absorption of the near-infrared wavelengths by water vapor, particularly near 750 and 900 nanometers, and (2) the unbalancing spectrally of exposure that results from the addition of energy by the upscatter of light of air luminance.

Air Luminance

Upscatter is spectrally selective according to the ratio of Rayleigh (λ^{-4}) to Mie (λ^0) scattering that is taking place. Rarely is air so pure that a λ^{-4} upscatter of energy exists (Brock et al, 1965). Conversely, all upscatter must include a component of Rayleigh scattering so that a λ^0 luminance would be similarly impossible. A wide variety of upscatter spectral curves between these two extremes can thus exist. When haze is heavy the amount of upscatter will be high and will approach a Mie curve. If haze is very light this contribution to overall exposure will be small and will approach a Rayleigh spectral distribution. Harvey and Myskowski

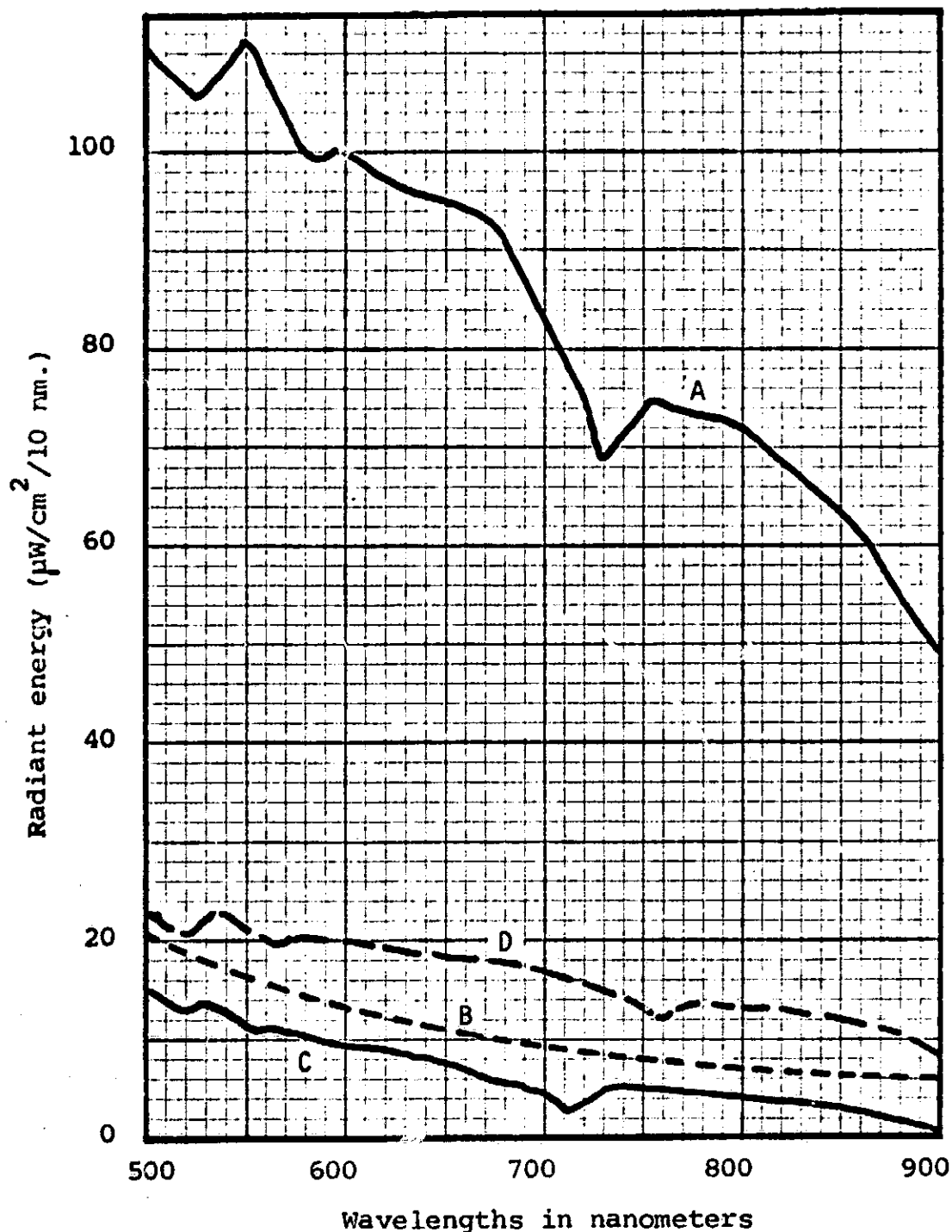


Figure 5. Upscatter of energy to high altitudes from air luminance. Upscatter of energy that will be added to the target reflection will be a portion of the incident solar illumination, modified according to the size of the molecules or particles doing the scattering. A typical solar curve (A) declines markedly toward the longer wavelengths. The dip at 750 nm. is due to water vapor absorption and will thus be present in the upscatter distribution. Curve B is a theoretical λ^{-2} distribution for a spectrally uniform illumination. It is included for comparison. Curve C is a $.08 \lambda^{-2}$ upscatter of curve A and thus drops more sharply toward the longer wavelengths than the theoretical curve B. Curve D is a $.20 \lambda^{-2}$ (Mie) distribution that also declines due to the solar curve it scatters.

(in Brock, et al, 1965) suggest that an λ^{-1} to λ^{-2} are probably most typical. With one exception, the following graphs use a λ^{-2} upscatter which represents a condition with little haze (Fig. 5).

The amplitude of the upscatter bears an important relationship to the exposure balance of the film. Experimental observation with a broadband spectroradiometer that measures in both the visual and near infrared spectral realms suggests that a λ^{-2} light haze condition returns approximately 8 percent of the incident illumination toward space. This is in agreement with observed values given in Brock (1965) for upscatter in the spectral band of 540-720 nm. In all likelihood λ^{-4} or pure Rayleigh scattering would be in the order of 5 to 6 percent, while luminance approaching a Mie condition would return 20 percent or more. Except for the example showing the unbalancing effect of pure Mie upscatter, a .08 return with a λ^{-2} distribution is used in the following graphs as being a typical luminance condition.

The Effect of Upscatter on Exposure Balance

Although a decrease in infrared exposure by water vapor absorption in the optical path is a factor working against a red infrared record at high altitudes, the additional exposure of air luminance can well be of greater importance. In Figure 6, the addition of a $.08 \lambda^{-2}$ upscatter to the pine needle reflection places the cyan density on the D log E diagram well above those of the other layers. The result will be a blue-green record for this target which records as red at close range. The upscatter added is that which would occur on a relatively clear day with little haze in the air. Only when the ratio of infrared to visual reflection strongly favors the infrared can a red record be obtained at

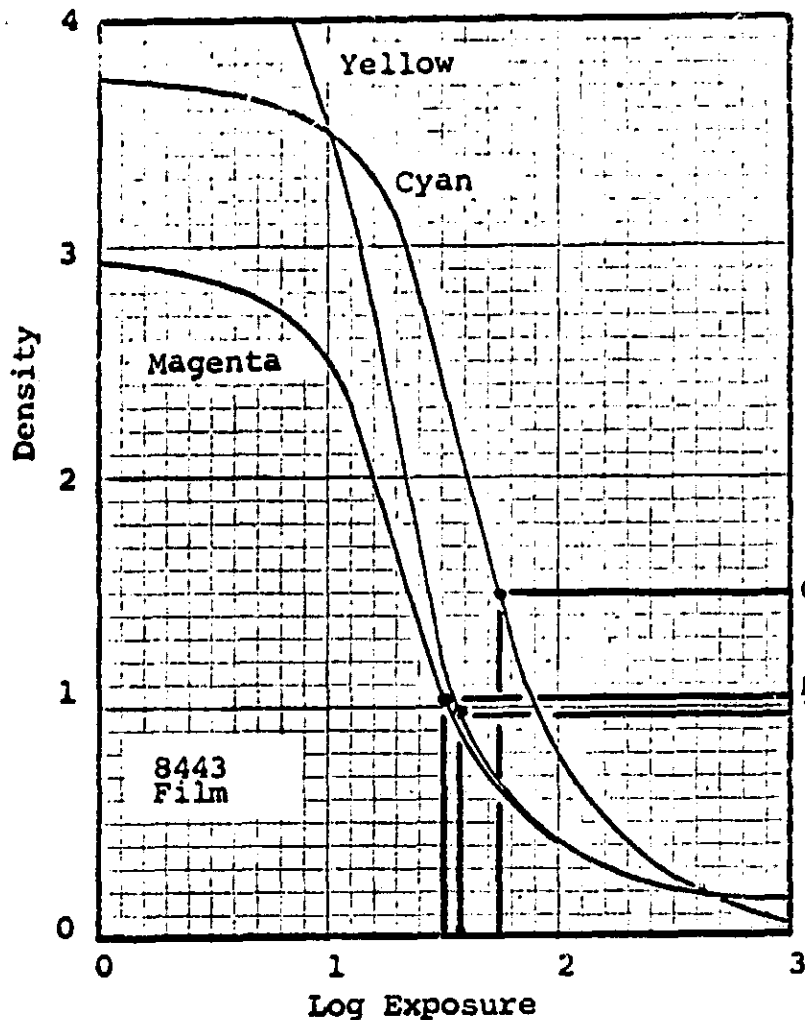
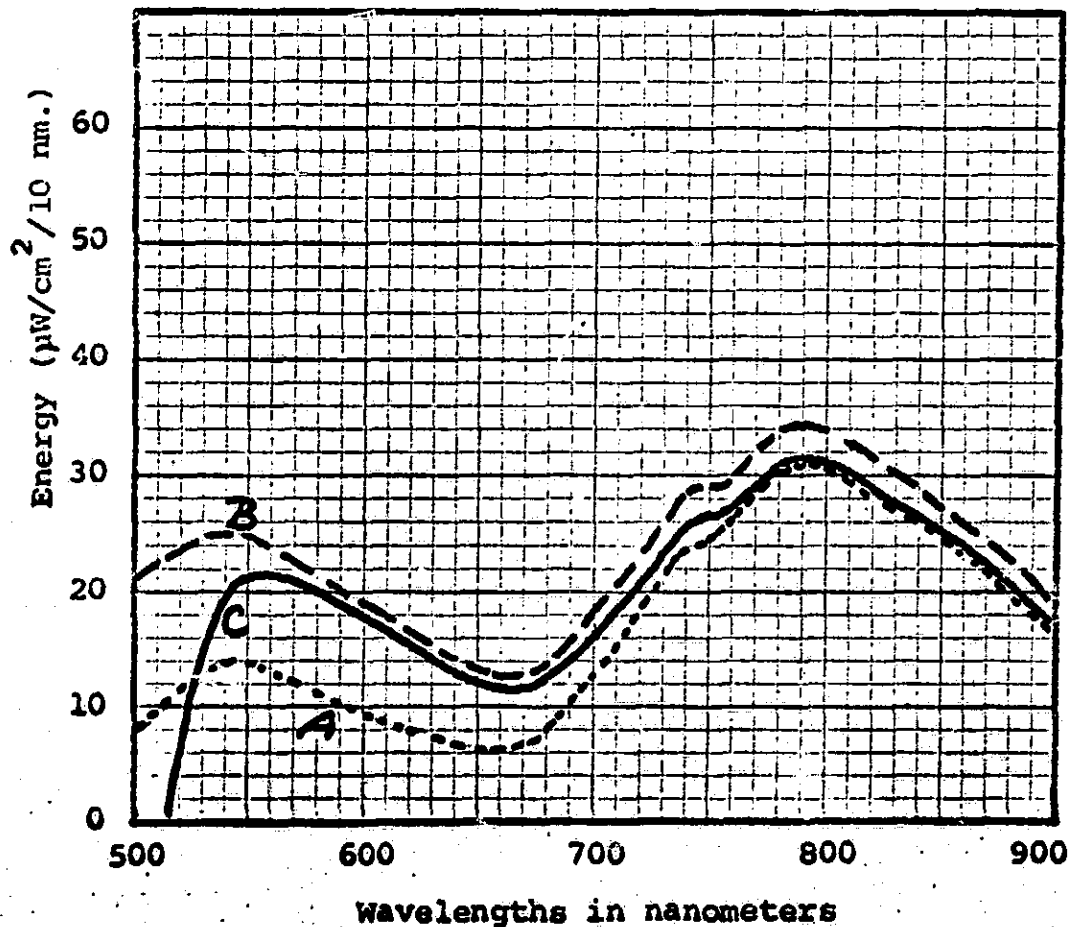


Figure 6. Pine needle reflection at high altitude, attenuated by water vapor in the IR, with $.08 \lambda^{-2}$ upscatter added to the exposure. Attenuation at camera by 15 filter.

A= 24.0 50.0 36.5 32.3 53.4 72.3 70.0 53.0



A=Pine needle reflection attenuated in IR by water vapor.

B=Reflection plus $.08 \lambda^{-2}$ upscatter.

C=Energy reaching film -- B attenuated by 15 filter.

high altitudes with the filtration recommended by the manufacturer of the film. Grass according to Fritz (1967) has close to an 8:1 IR/Visual reflectance ratio, which when plotted (Fig. 7) gives a cyan density slightly below that of the other layers. This would produce a dark or unsaturated red record on the transparency.

The fact that λ^{-2} upscatter adds more energy to the shortwave end of the CIR exposure spectrum than to the long wave end causes it to have a marked effect in changing the spectral exposure balance. However, a pure Mie (λ^0) upscatter, if such were theoretically possible, would be similarly effective. The $.20\lambda^0$ upscatter of energy added to the pine needle reflection in Figure 8, by building up exposure energy in all wavelengths, reduces the spectral contrast in a manner similar to the reduction of scene contrast by air luminance. As is illustrated, this will reduce the IR/Visual exposure ratio and cyan density will predominate. It should be noted that a λ^0 curve will decline at its longwave end when it upscatters sunlight.

The Use of Minus-Visual Filters

The effects on exposure balance wrought by water vapor attenuation and the addition of air luminance or upscatter can be offset by the use of filters that attenuate the visual wavebands but not the near infrared. Several dye filters which essentially do this have been described by Pease and Bowden (1968). When these are used as auxiliaries to the basic minus-blue filter, spectral transmittance characteristics remold by selective attenuation the energy curve reaching the camera. Curve B in the spectral energy plot of Figure 9 indicates the energy reaching the film after it has

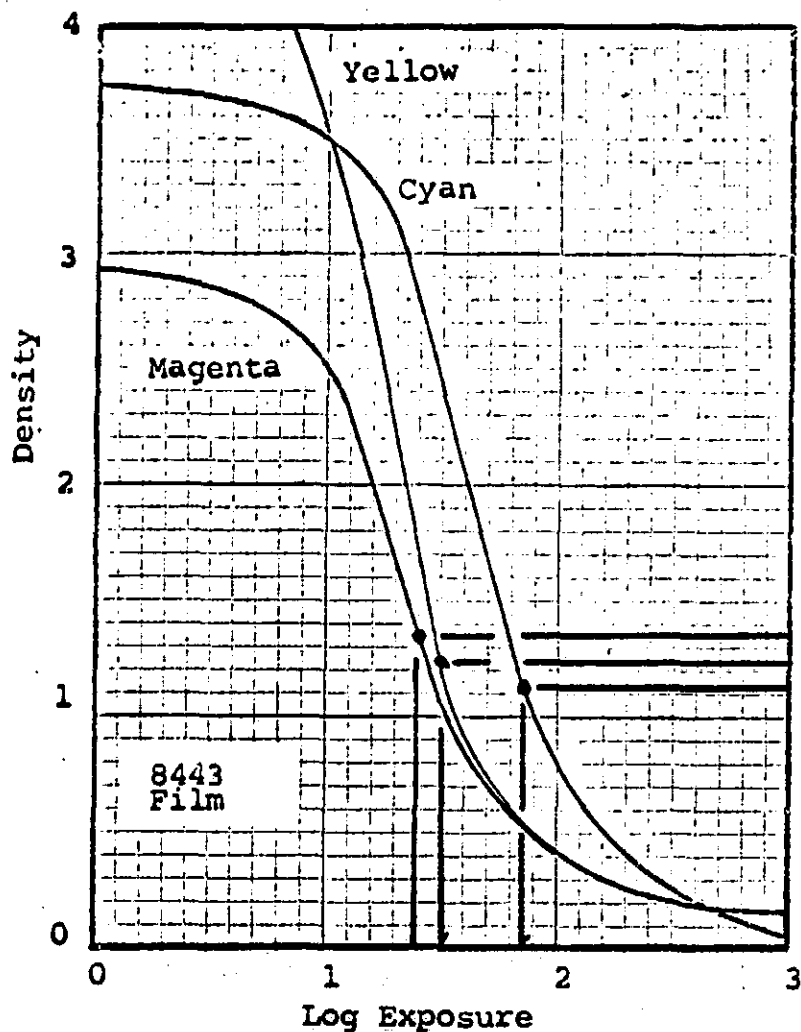
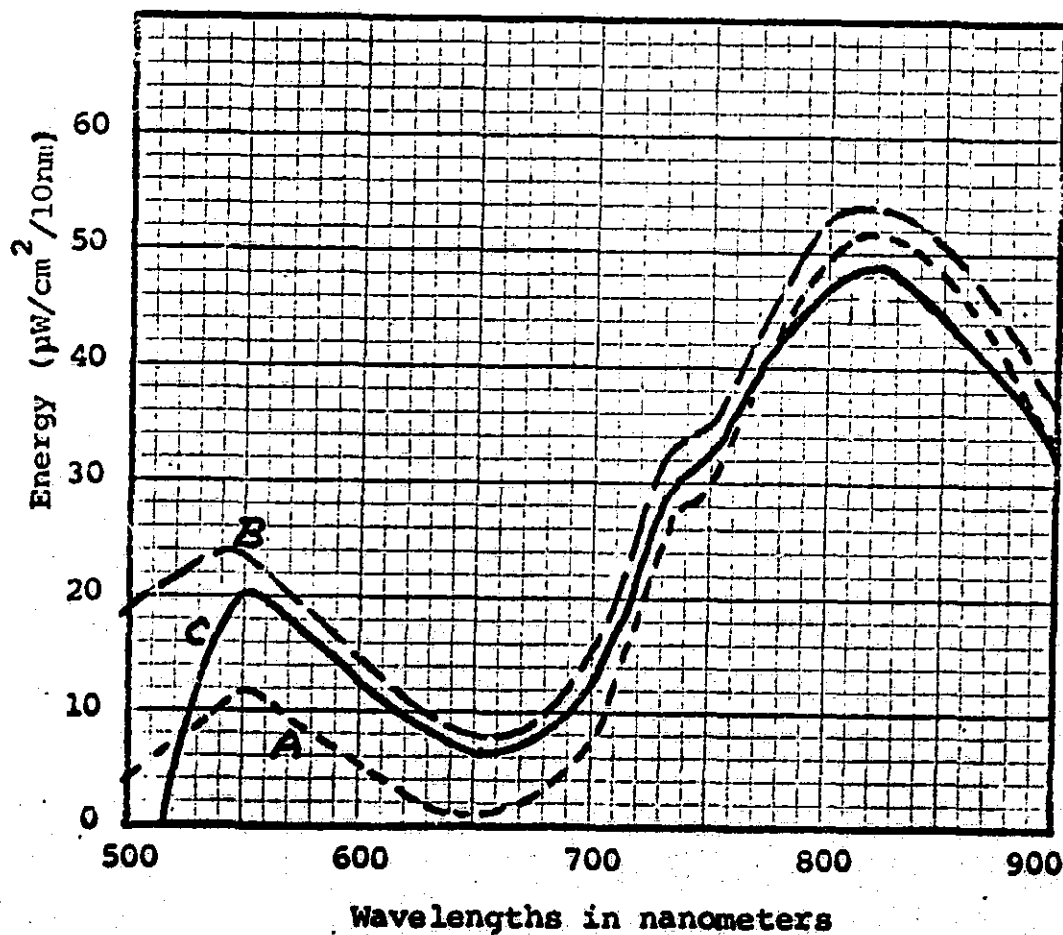


Figure 7. A high IR reflectance target (grass) at high altitude. For this target a dark red would show. The grass reflectance is according to Fritz (1967). Only a 15 filter is used with the camera.

A= 21.2 42.0 22.0 19.5 60.0 99.0 113.5 95.0



A=Plant reflection.
 B=Reflection plus .08 λ^{-2} upscatter.
 C=Energy reaching film -- B attenuated by 15 filter.

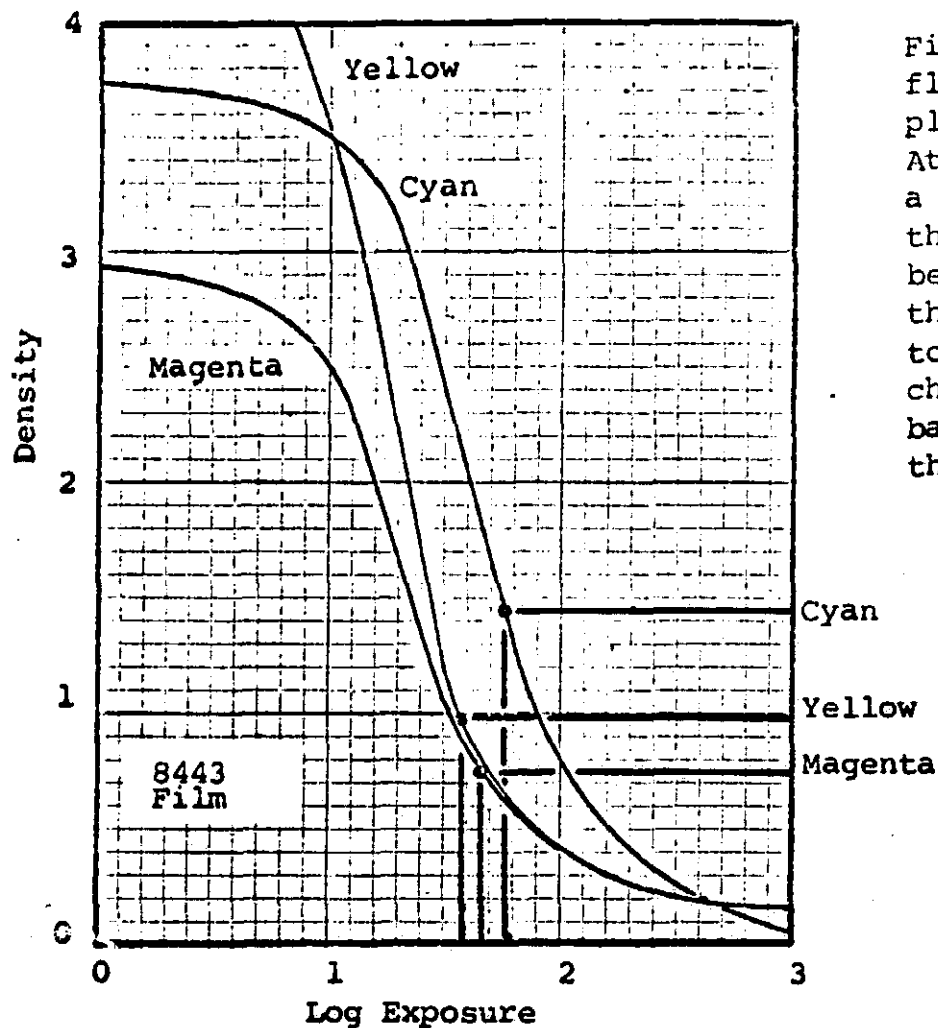
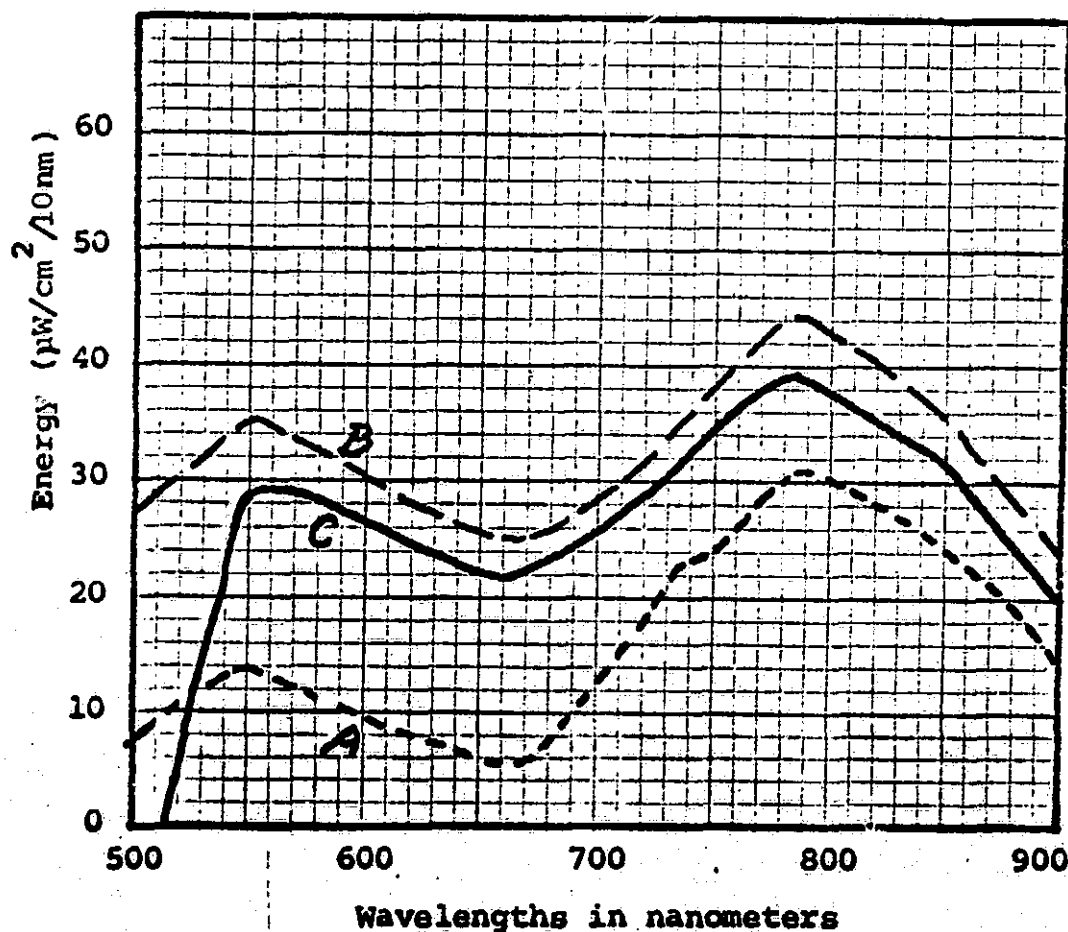


Figure 8. Pine needle reflection at high altitude plus a λ° (Mie) upscatter. Attenuation at camera is a 15 filter only. Although the upscatter is close to being spectrally neutral, the addition of this light to the target reflection changes the visual-infrared balance of light reaching the camera.

A= 26.5 70.0 60.2 58.0 72.5 93.3 86.0 63.2



A=Pine needle reflection, attenuated in IR by water vapor.

B=Reflection plus .20 λ° upscatter.

C=Energy reaching film -- B attenuated by a 15 filter.

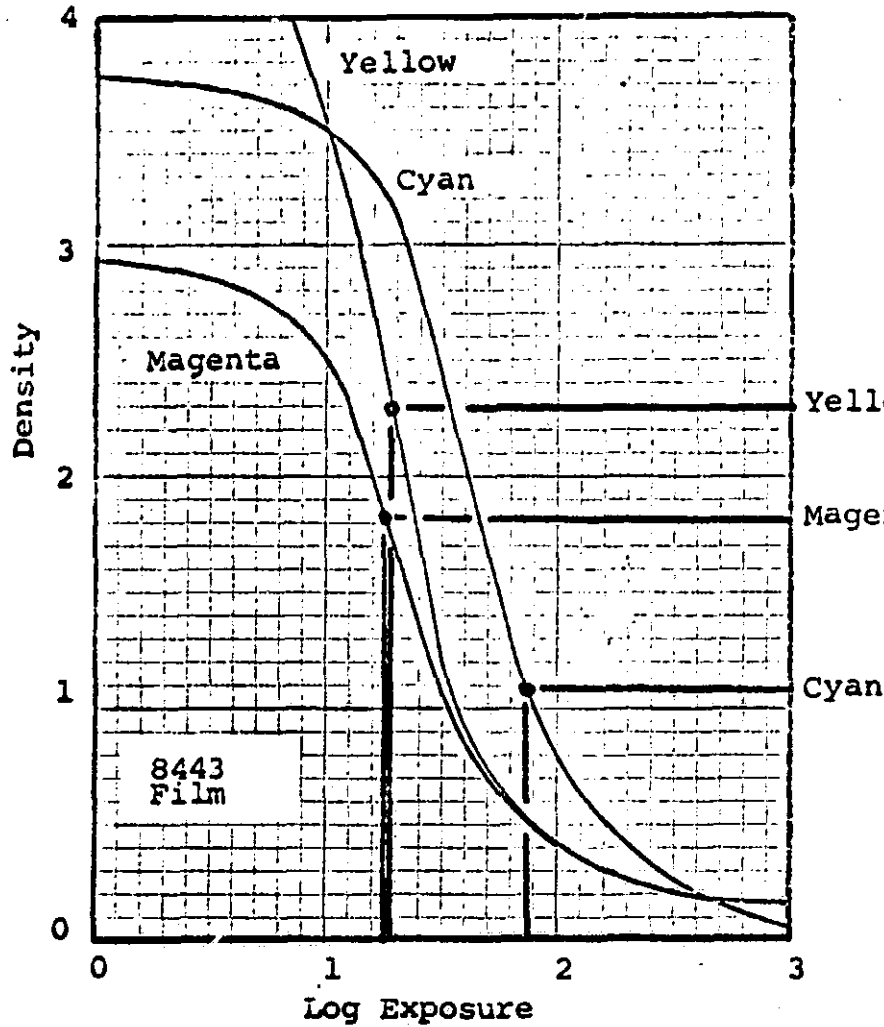
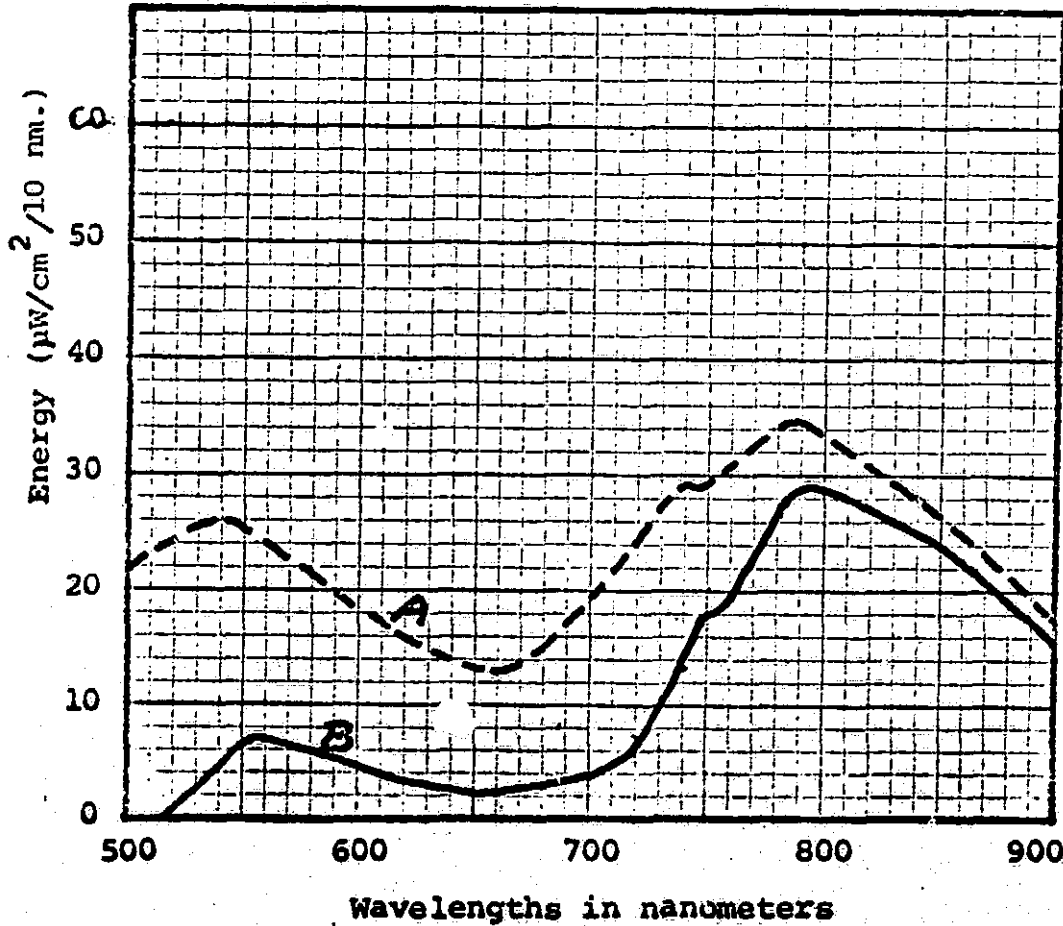


Figure 9. Pine needle reflection at high altitudes with a minus-visual (80B) filter. Upscatter is $.08 \lambda^{-2}$. By remolding the energy reaching the camera with the spectral transmittance of the 80B filter, the cyan density is rendered far lower than the densities of the other Magenta dye layers.

A= 4.6 14.5 8.0 7.0 22.5 60.0 66.0 50.0



A=Reflection plus upscatter at high altitude.

B=Energy reaching film -- A attenuated by 15 and 80B filters.

been attenuated by the 15 and an 80B filters. Attenuation in the visual band is sufficiently strong that again the relative infrared exposure will yield a cyan density lower than the yellow or magenta. In fact the cyan is lower than is the case with a 15 filter alone at close range. With the yellow denser than magenta, the IR record is an orange-red.

Not all components of the image are vegetation targets, however. Many urban targets, for example, are close to neutral, with a nearly equal reflectance to all wavelengths of the CIR spectrum. Figure 10 plots a .15 reflectance neutral target photographed at close range. Even though the target has a constant reflectance, there is a measure of decline toward the IR end due to the solar illumination curve it reflects. When the neutral target reflection plus upscatter are remolded by an 80B filter, cyan still predominates, but to a lesser degree (Fig. 11). The result is a blue-gray hue which experience has shown to be characteristic for urban targets when an 80B filter is used.

Soil and weathered rock surfaces are important components of non-urban images. For these, a reflectance that rises steadily from the visual into the infrared appears to be typical. Although this built-in IR exposure advantage is insufficient to prevent a cyan dominance when only a 15 filter is used, 80B attenuation lowers the cyan density to approximately that of the other layers and neutral tones ensue (Fig. 12). An 80B rather drastically attenuates the energy in the visual wavelengths. It can thus maintain neutral soil tones even at high altitudes as is illustrated by Figure 13. Minus-visual filters which attenuate the visual wavelengths less than the 80B do not yield neutral tones at high altitude from soil targets. This is

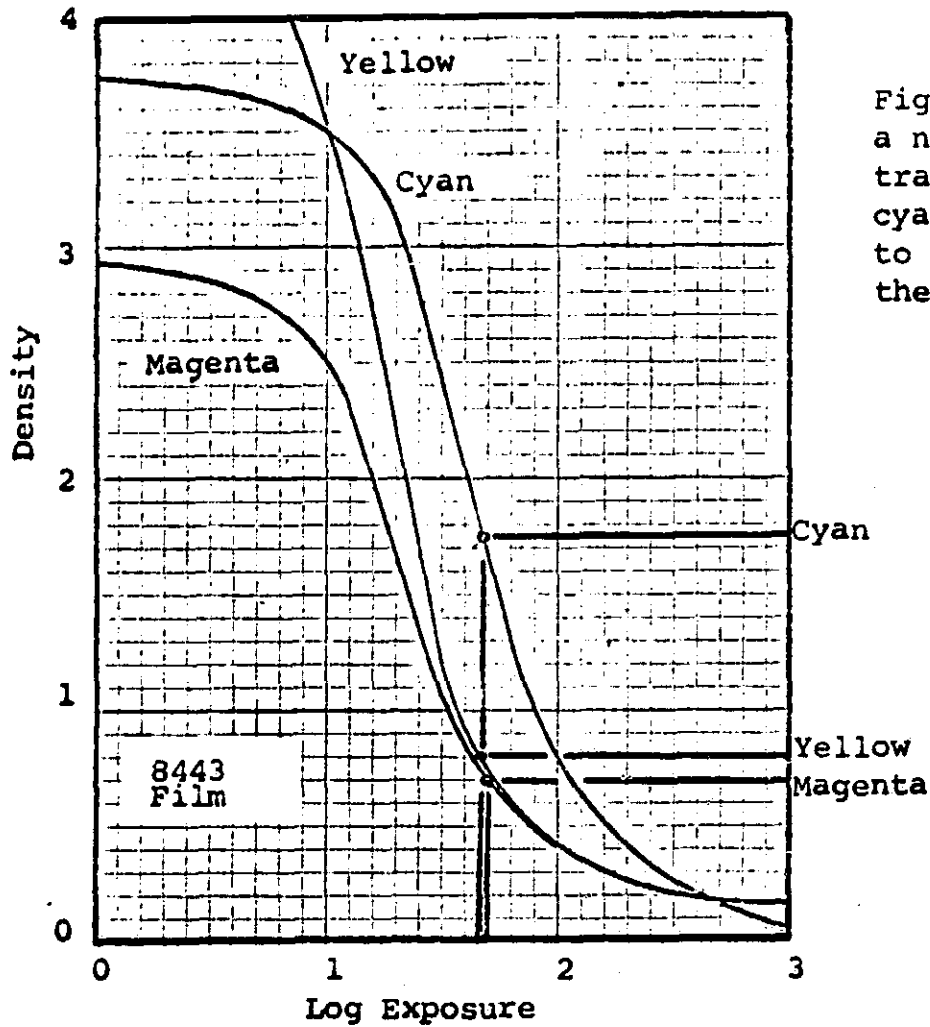
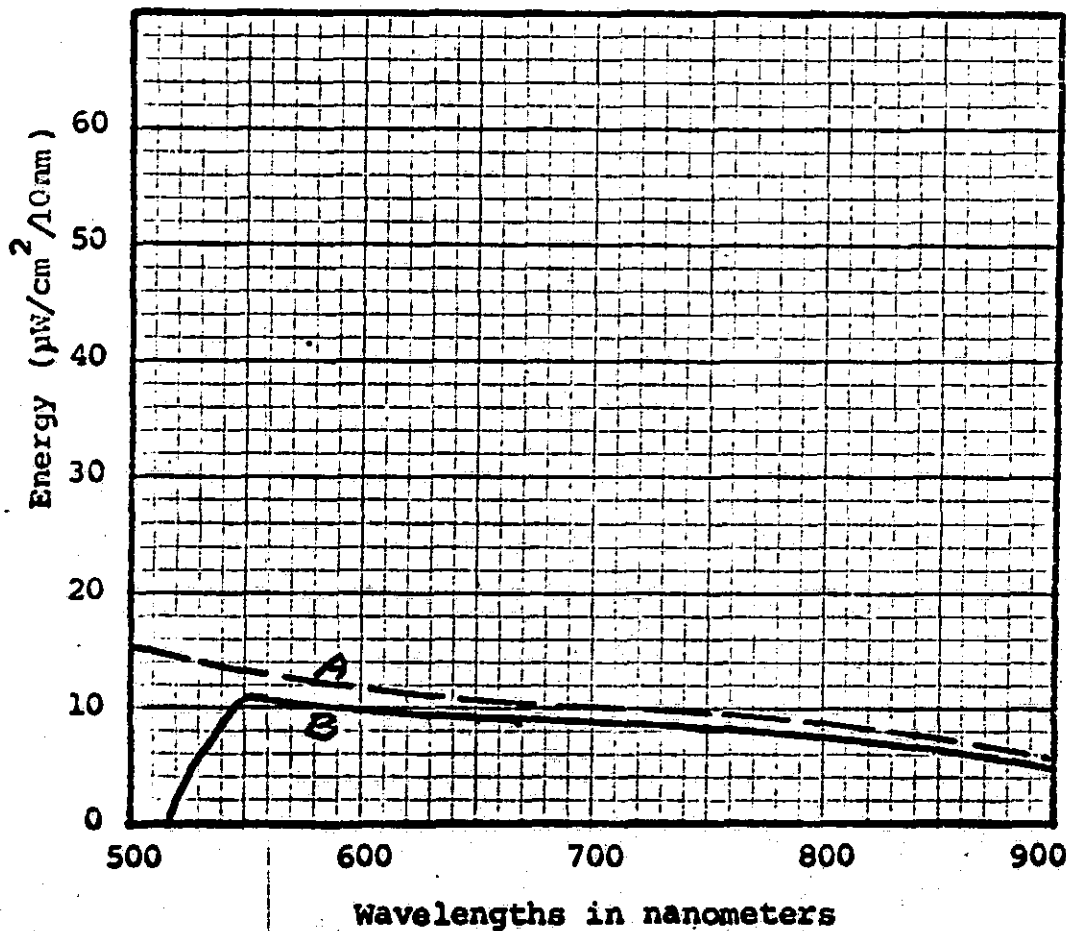


Figure 10. Reflection from a neutral target. For neutral targets at close range cyan must predominate due to the lower sensitivity of the layer.

A= 10.0 25.5 24.0 22.5 21.5 19.7 16.3 13.6



A=Reflection from .15 neutral target in sunlight.

B=Energy reaching film -- reflection attenuated by a 15 filter.

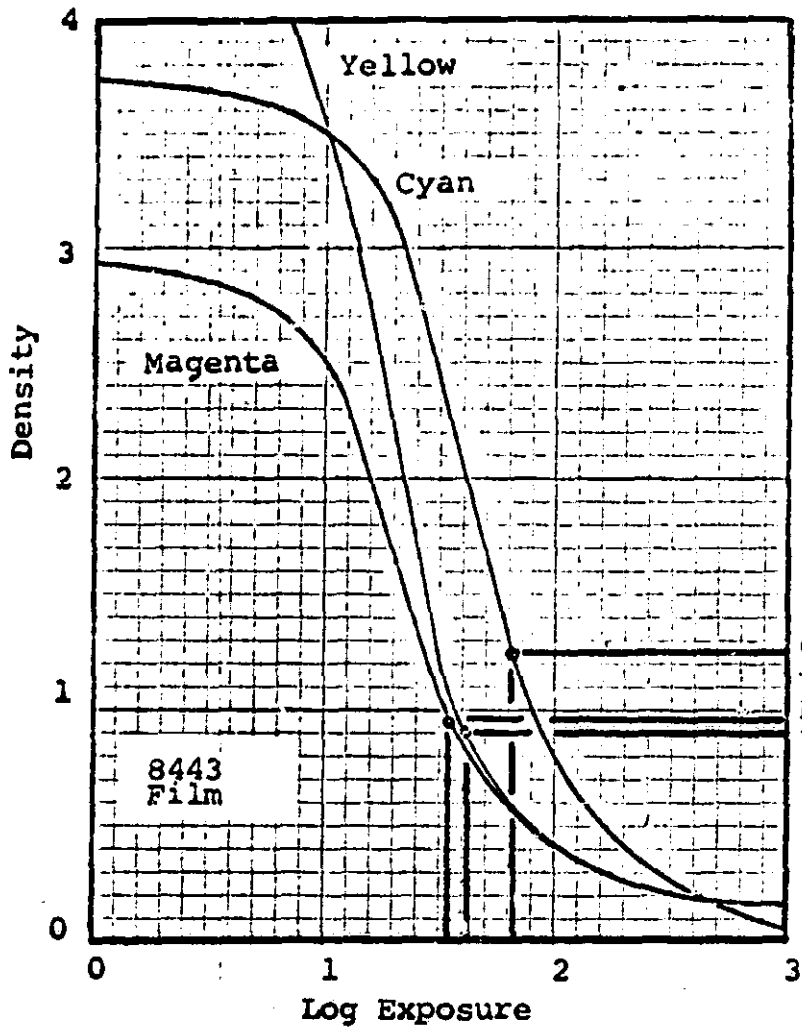
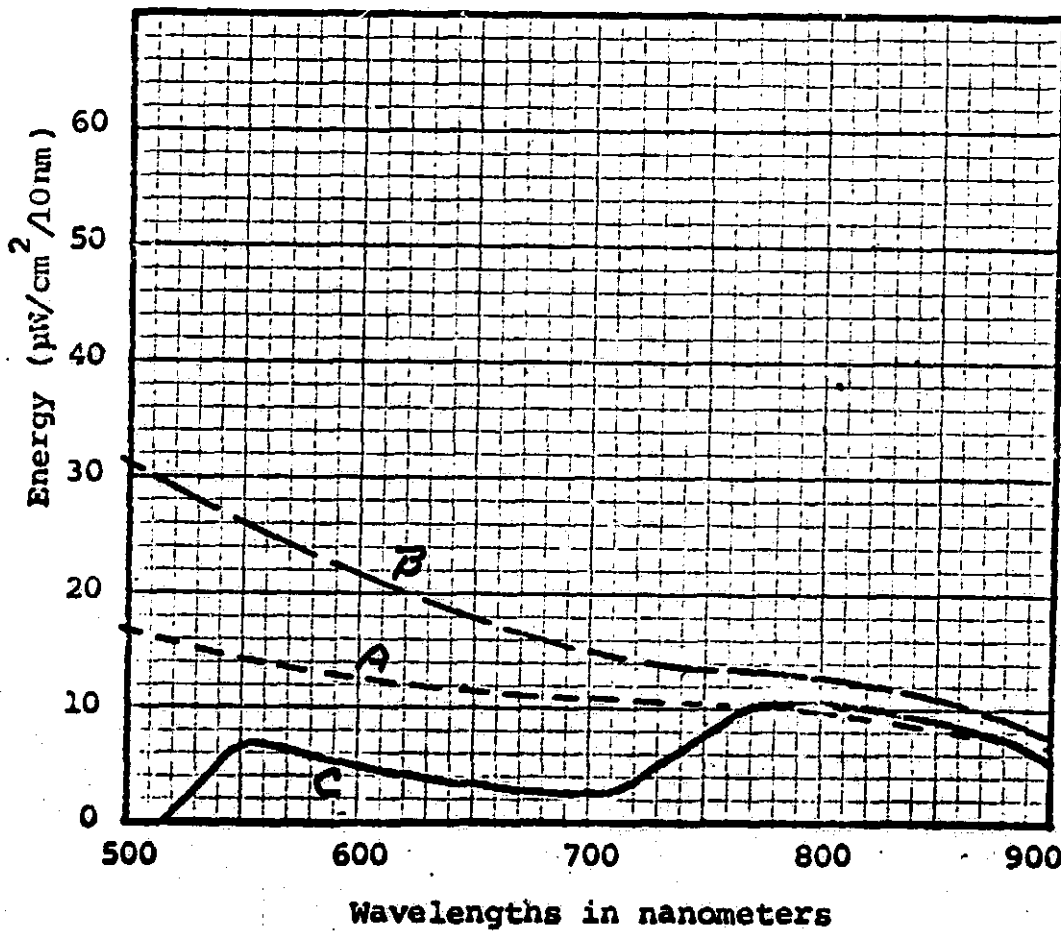


Figure 11. Reflection from a neutral target at high altitude, using 15 and 80B attenuating filters. The dye layer balance is close to neutral but with a moderate cyan dominance. This yields the characteristic blue-gray tones typical for many urban targets, such as concrete, blacktop, and dusty roofs.

A= 5.0 14.5 9.5 6.0 11.0 24.0 24.2 18.4



A=Reflection from a .15 neutral target in sunlight.
 B=Reflection plus a $.08 \lambda^{-2}$ upscatter.
 C=Energy reaching film -- B attenuated by 15 and 80B filters.

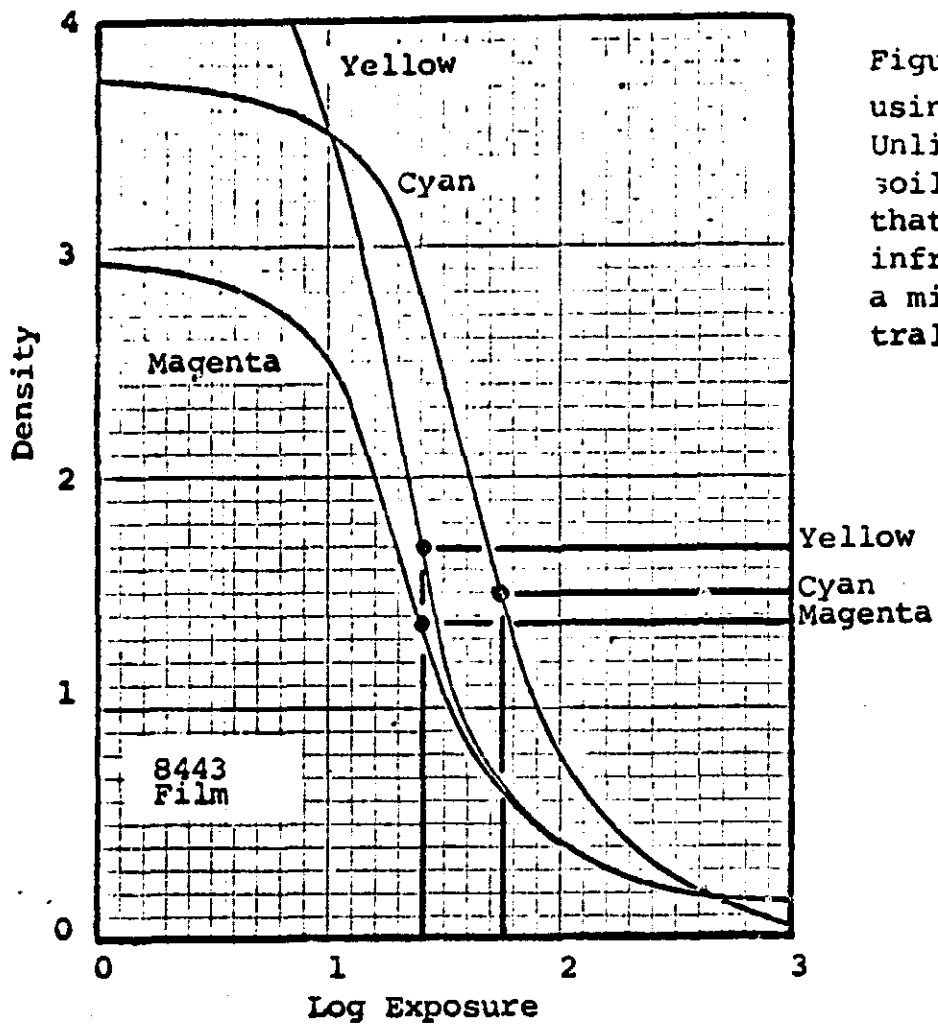
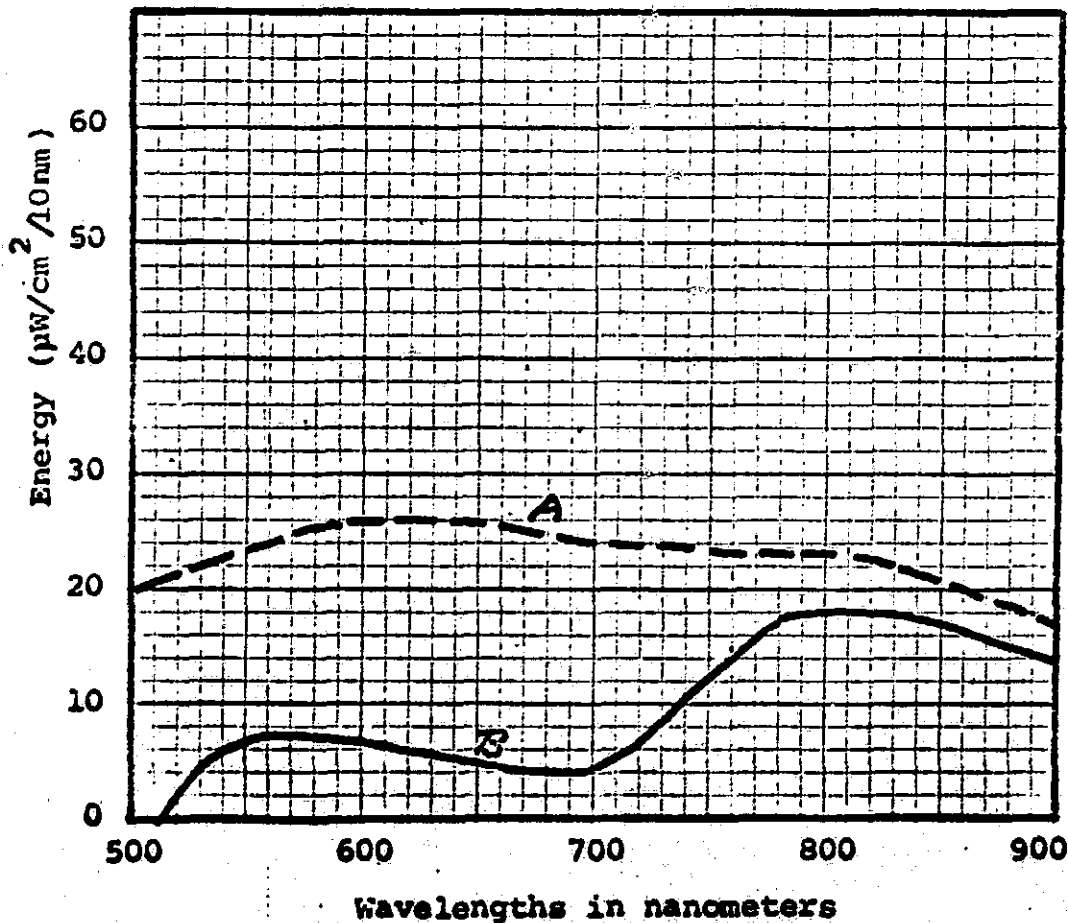


Figure 12. Soil at close range using a 15 and 80B filter. Unlike truly neutral targets, soils often have reflectances that rise markedly in the infrared. With an 80B as a minus-visual filter, neutral tones are obtained.

A= 7.5 17.0 14.0 10.0 18.0 40.0 44.5 38.2



A=Reflection of weathered granite with sunlight illumination.
B=Energy reaching film -- A attenuated by 15 and 80B filters.

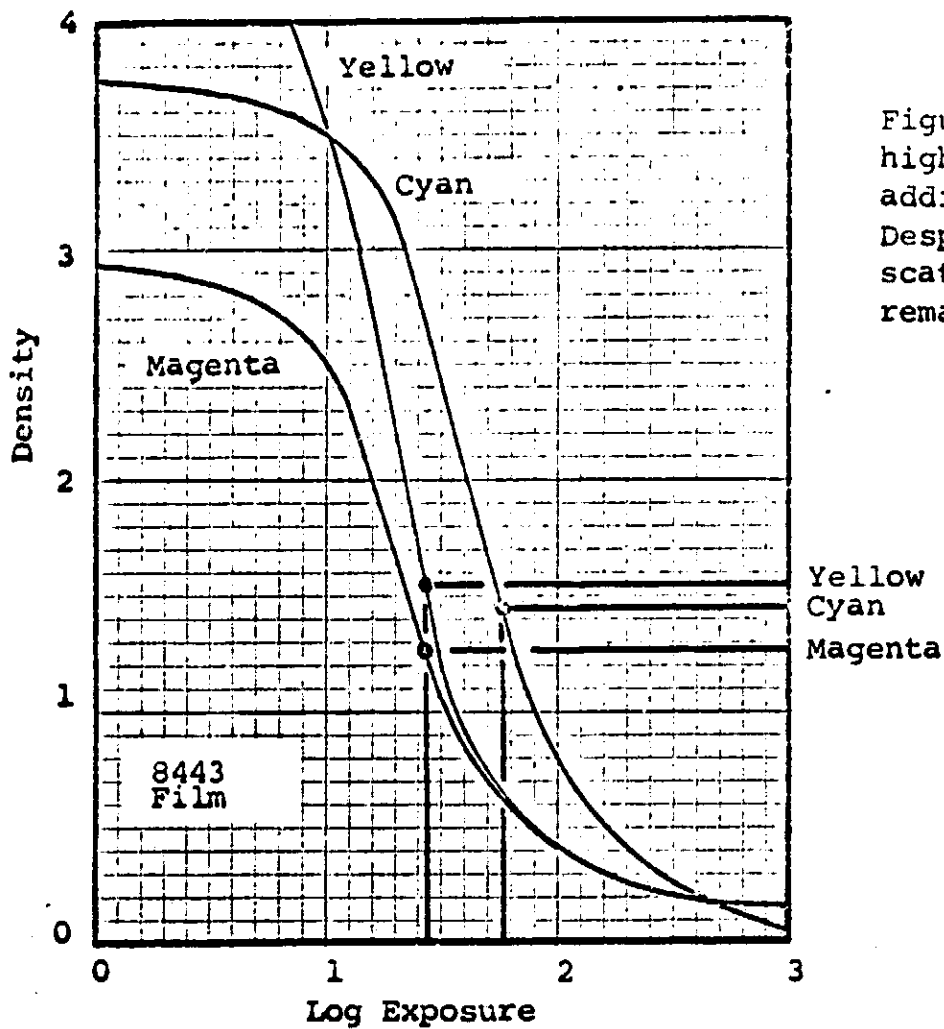
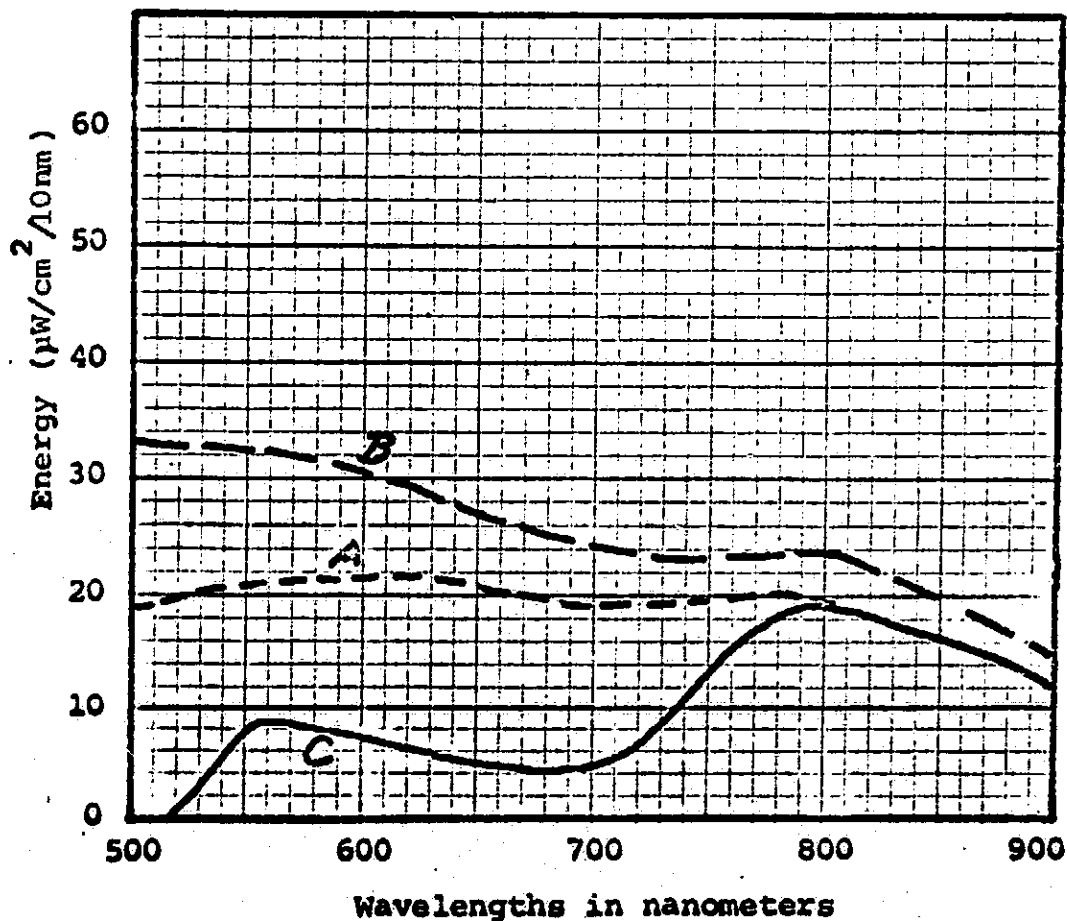


Figure 13. Soil reflection at high altitude using an 80B in addition to the 15 filter. Despite the addition of up-scatter, the dye layer balance remains close to neutral.

A= 5.6 20.0 14.5 10.6 20.0 42.2 44.0 36.0



A=Soil reflection under sunlight.
 B=Reflection plus $.08 \lambda^{-2}$ upscatter.
 C=Energy reaching camera -- B attenuated by 15 and 80B filters.

illustrated by Figure 14 where a CC30B is used at the camera in conjunction with the 15. Cyan predominates in density, but yellow is strong. With this combination, soil and weathered rock targets appear a true green rather than the blue-green cyan that occurs when a 15 is used alone or the neutral tones obtained with an 80B.

SUMMARY

The foregoing describes a method whereby the relative dye layer densities of Type 8443 color infrared transparency film can be predicted. In so doing it quantitatively substantiates existing experience with the use of minus-visual filters for combating the effects of high altitude. An obvious next step is the transformation of the relative dye layer densities into actual color hues and tones.

Although there is no attempt here to provide a precise method for this color synthesis, subjective evaluations can be made. First, it is necessary for the cyan density to be lower than those of the other two layers for a red record to show. Since the cyan, or the lack of it, only provides the window through which the red color shows, it is necessary that the magenta and yellow have sufficient density to yield in concert the desired red. Second, the lowest density will set the neutral density or tone level of the color. If this is high, the overall tone will be dark. If this is low, the overall tone may be light. The departure of the other two densities from that of the lowest density can be considered as setting the color hue. If the neutral level is low, but the other densities are high, bright colors will result. If conversely, the neutral level is high and departure from this is only slight, dark unsaturated colors will result.

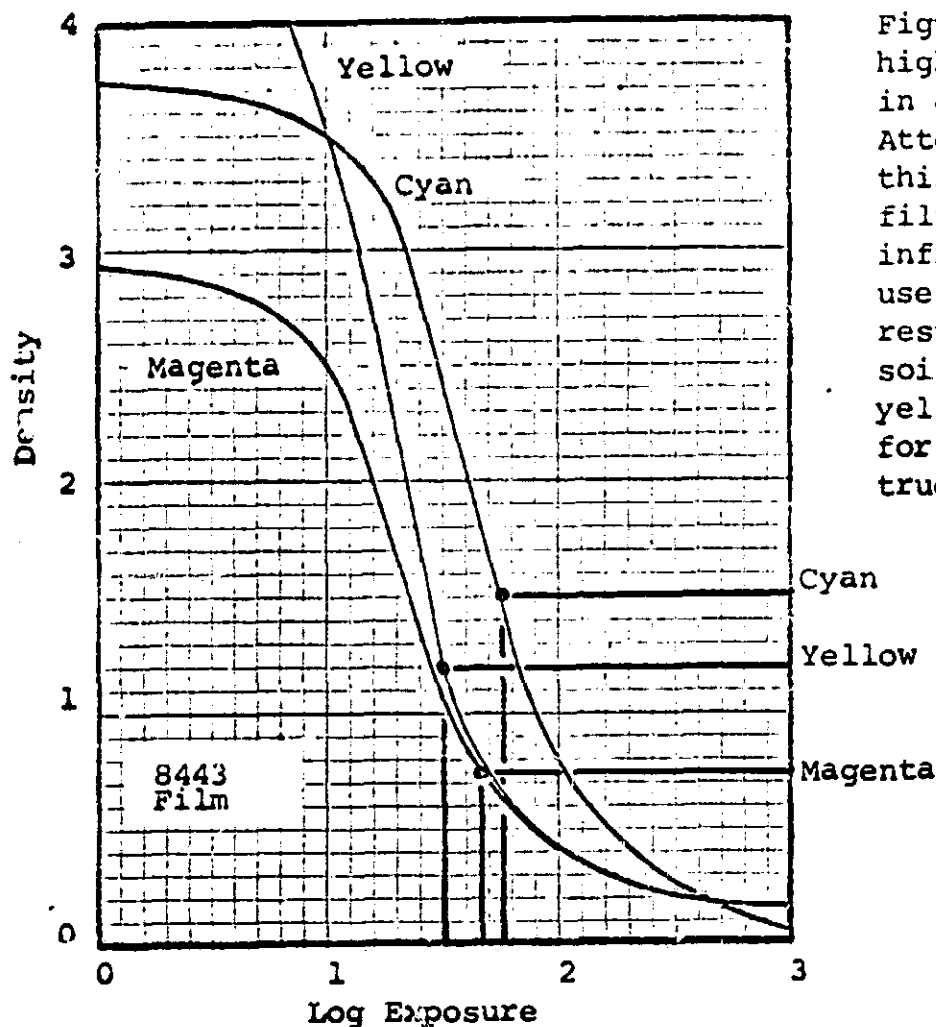
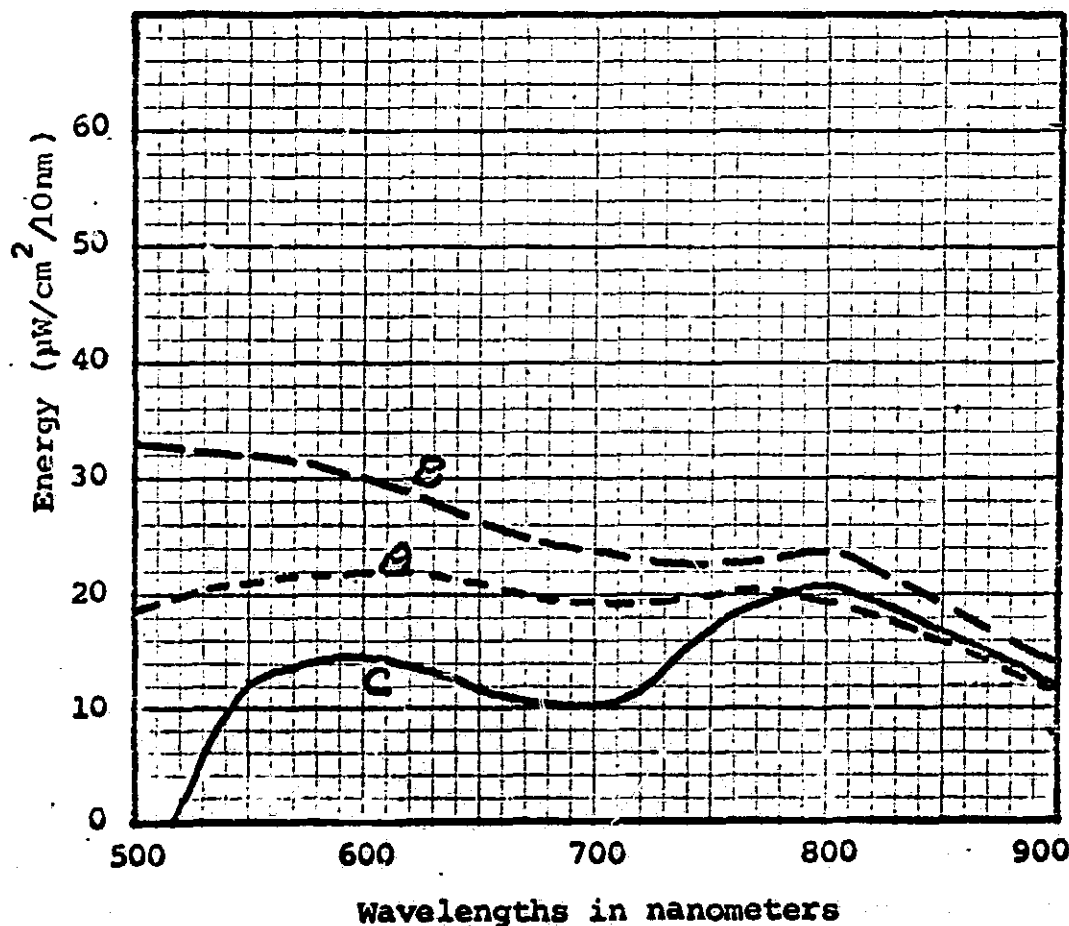


Figure 14. Soil reflection at high altitude using a CC30B in addition to the 15 filter. Attenuation at the camera by this minus-visual auxiliary filter does not favor the infrared exposure as much as use of the 80B does. The result is a cyan dominance for soil targets, but with a strong yellow density. The general hue for soil and rocks is thus a true green.

A= 10.5 34.0 33.0 26.0 32.5 48.0 47.2 36.0



The two denser layers will set the color hue in proportion to their departures from the neutral density level. Should they be equally dense, the hue will divide between them, more frequently one dominates and the combination will favor the densest. These guideline can be helpful in evaluating hue.

cyan + magenta → blue to purple

magenta + yellow → red

cyan + yellow → green

There are color systems whereby the tone and hue can be pinpointed with greater accuracy. The Munsell system is one. It is intriguing to consider that the process can be reversed. By matching a Munsell slip to a color on a transparency, the reflectance curve for the target can be ascertained when the conditions under which the images were made are known.

BIBLIOGRAPHY

Brock, G.C., et al, 1965, Photographic Considerations for Aerospace. Itek Corporation, Lexington, Mass. 122 pp.

Fritz, Norman L., 1967, "Optimum Methods for Using Infrared-Sensitive Color Film," Photogrammetric Engineering, Vol. XXXIII, Number 10, (October) pp. 1128-1138.

Pease, R.W. and Bowden, L.W., 1968 "Making Color Infrared Film a More Effective High Altitude Remote Sensor," Remote Sensing: an Interdisciplinary Journal, Vol. 1 (in press).

Also issued as: Technical Letter NASA-117, May 1968, Manned Spacecraft Center, Houston, Texas.

Tarkington, R. and Sorem, A., 1963, "Color and False Color Films for Aerial Photography," Photogrammetric Engineering, Vol. XXIX, Number 1 (January) pp. 88-95.

ADDENDUM

--

COLOR INFRARED PHOTOGRAPHY THROUGH SPACECRAFT WINDOWS

All glass becomes opaque to long wavelengths of radiant energy. For most, significant decline in transmittance occurs at wavelengths far longer than those within the CIR spectrum. Spacecraft windows or ports, however, may have heat-shielding coatings which interfere with the transmission of the infrared energy that exposes the cyan-forming layer of color infrared film.

Two transmittance curves for spacecraft ports are shown in Figure 15. Curve A is described as being at an angle of incidence of 45° to the window and thus is assumed to be an off-axis condition. There is no stipulation for the angle through which measurements were made for curve B, purportedly the same window.

In predicting the densities of CIR dye layers of photographs taken through them, the windows are simply considered as additional attenuating filters. The ground target is the previously used pine needles to the reflection of which is added $.08 \lambda^{-2}$ air luminance.

For curve A the transmittance drops so rapidly above 700 nm. that much of the exposure of the cyan-forming layer is lost. The use of minus-visual auxiliaries does not help since their rise in transmittance almost exactly is cancelled by the increasing opacity of the window. For the plotting in Figure 16 a Wratten 22 was used as the minus-blue filter to decrease the exposure in the visual realm. A 78B filter was used to attenuate the visual wavelengths since its peak density occurs at a somewhat shorter

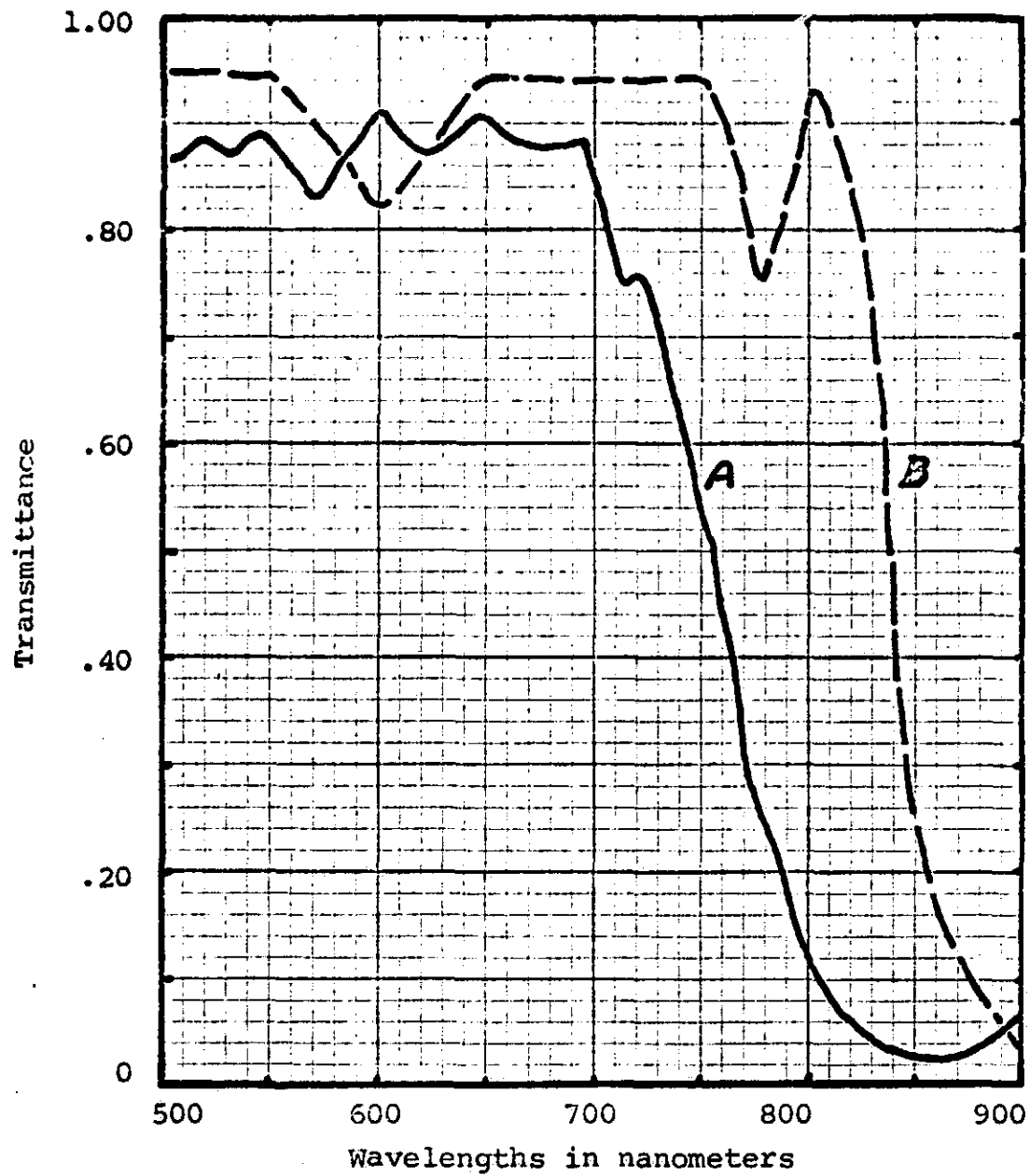


Figure 15. Transmittances of heat-shielded spacecraft windows or ports. Curve A, furnished by North American, is described as "45° incidence." Curve B, supplied by MSC has no such stipulation.

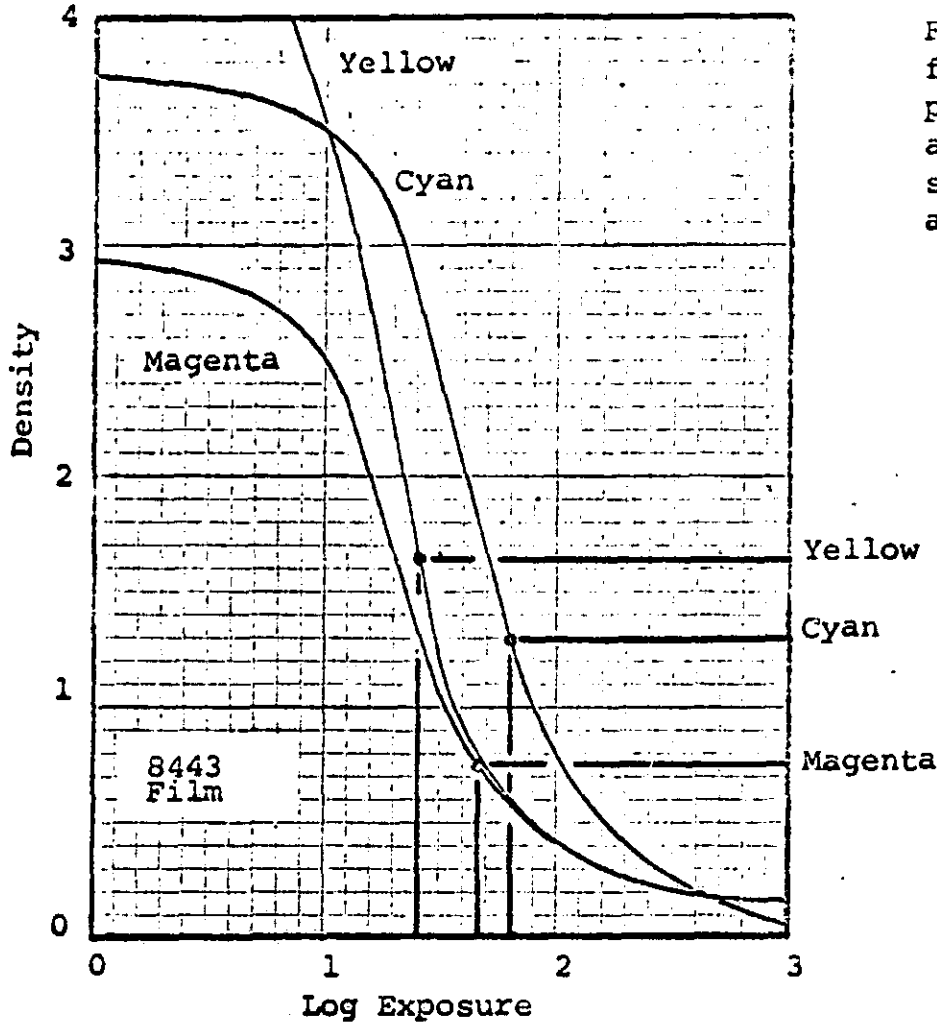
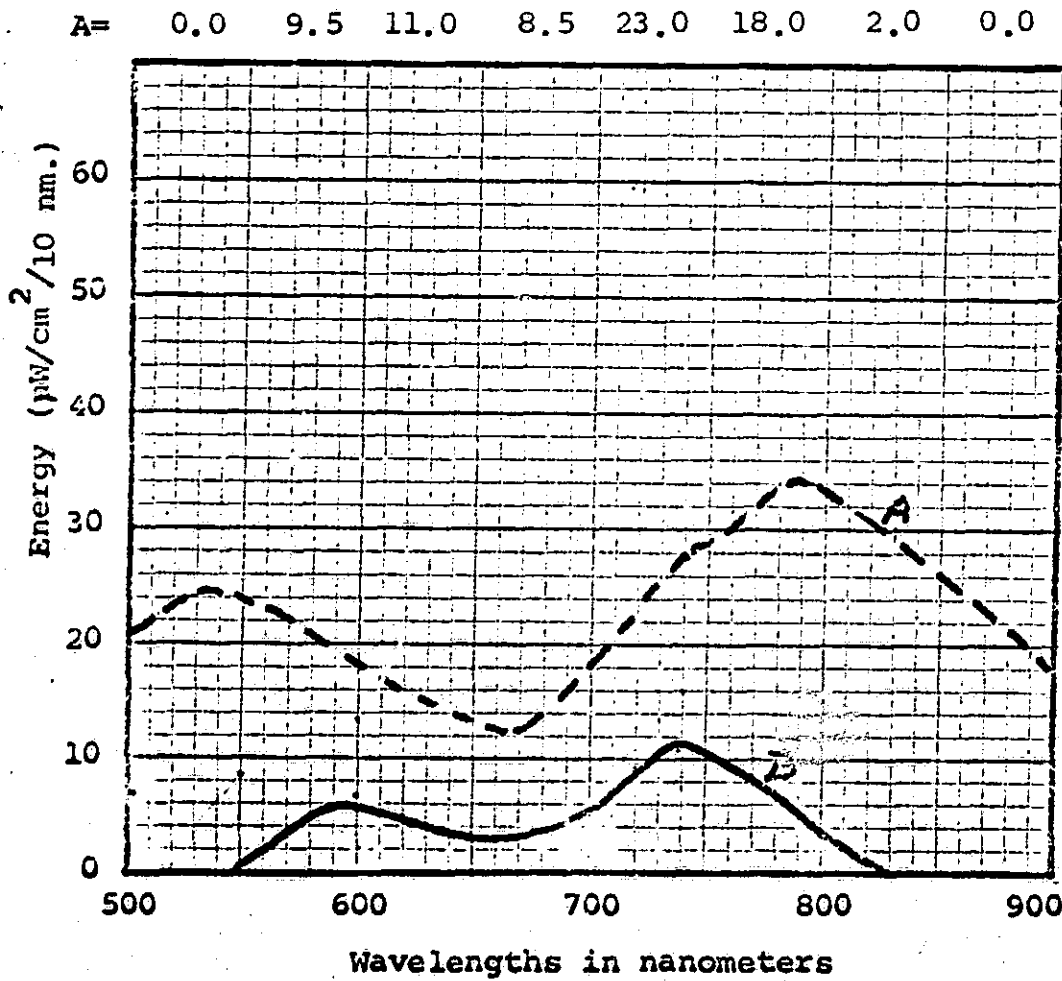


Figure 16. Pine needle reflection at high altitude plus an $.08 \lambda^{-2}$ upscatter, attenuated by a curve B spacecraft window and 22 and 78B camera filters.



A= Reflection plus upscatter as it reaches spacecraft.

B= Energy at film-- A attenuated by port, 22, and 78B filters.

wavelength (650 nm.) than the 80B (700 nm.). Despite these precautions there is insufficient exposure of the cyan layer to give a density lower than that of the other layers. No red record could result from this target, although a high IR reflectance target such as grass might yield a purplish red color.

The transmittance of port B will yield a good red record of the pine needle target with the 15 as the basic minus-blue filter and a 78B as the minus-visual auxiliary. This is demonstrated in Figure 17 where the cyan density is substantially lower than that of the other layers. Enough infrared exposure is available through this window that an 80B should also be a successful auxiliary, yielding only a slightly less red result than the 78B.

Pine needles have a relatively low IR/Visual reflectance ratio. Other targets such as grass in its vegetative stage, broadleaf forest, or most leafy crop plants would yield a brighter red. It can thus be concluded that with moderately clear conditions, color infrared photography through a port with a curve B transmittance would be quite successful, provided an appropriate minus-visual auxiliary filter such as the 78B or the 80B is used to combat the effects of high altitude.

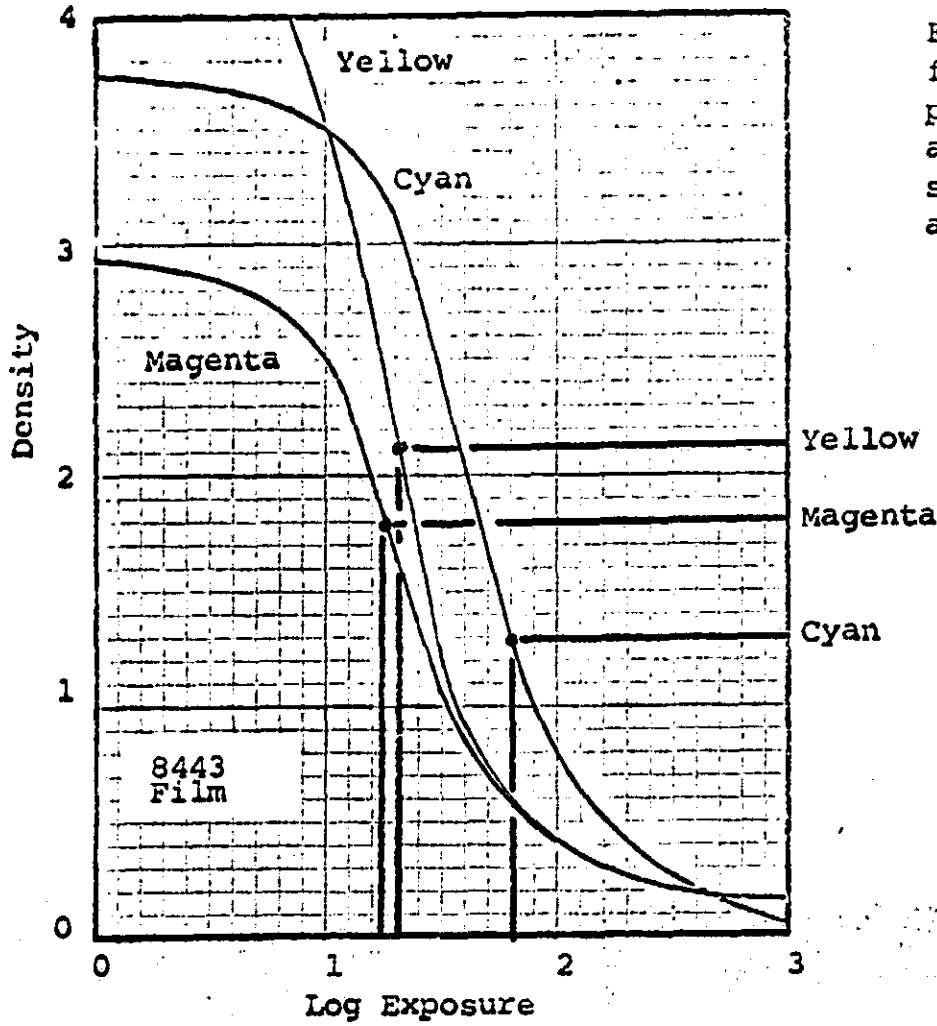
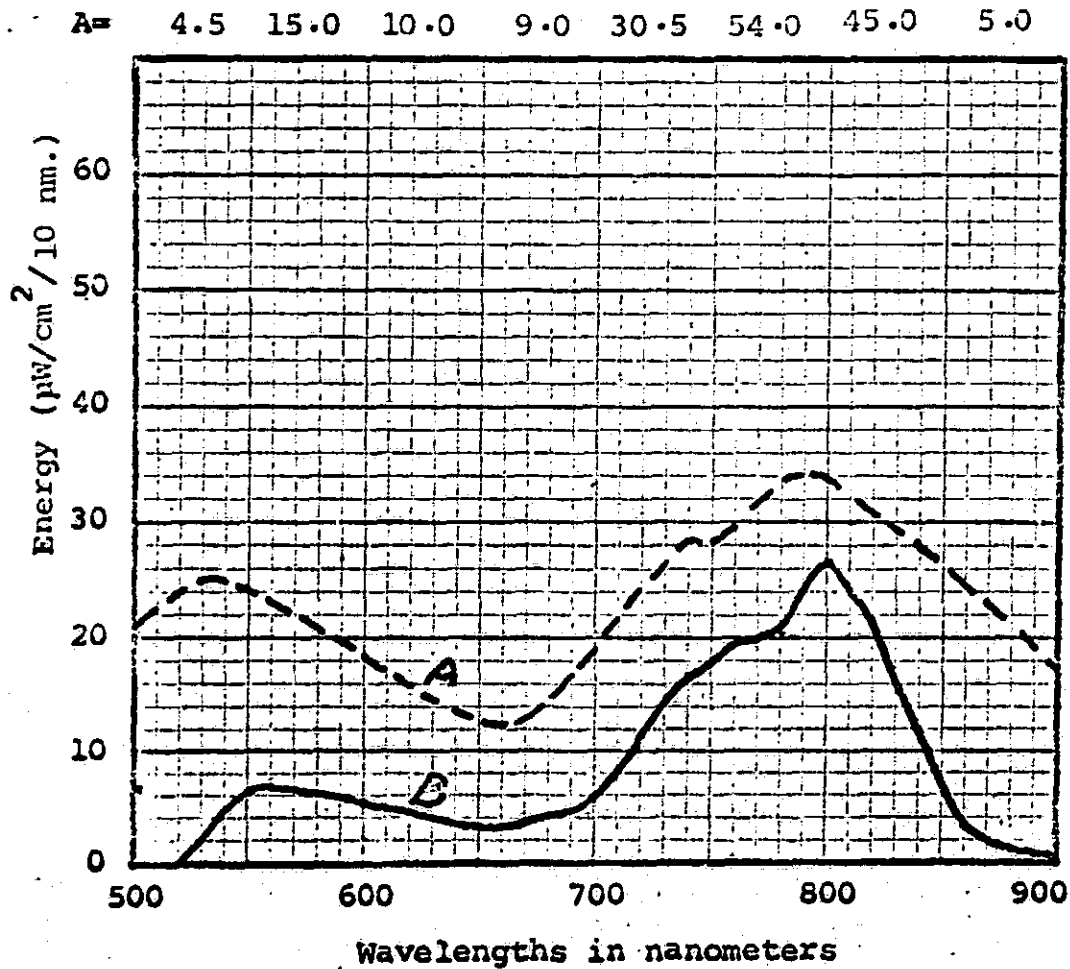


Figure 17. Pine needle reflection at high altitude plus an $.08 \lambda^{-2}$ upscatter, attenuated by a curve B spacecraft window and 15 and 78B camera filters



A=Pine needle reflection attenuated by water vapor plus $.08 \lambda^{-2}$ upscatter.
 B=Energy at film-- A attenuated by curve B transmittance port, 15, and 78B filters.